Sidechain conformational distributions of a small protein derived from modelfree analysis of a large set of residual dipolar couplings

Fang Li,[1,2] Alexander Grishaev,[3] Jinfa Ying,[1] and Ad Bax[1,*]

[1] Laboratory of Chemical Physics, National Institute of Diabetes and Digestive and Kidney Diseases, National Institutes of Health, Bethesda, MD 20892, USA

[2] Key Laboratory of Pesticides and Chemical Biology, College of Chemistry, Central China Normal University, Wuhan, Hubei 430079, People's Republic of China

[3] National Institute of Standards and Technology, Institute for Bioscience and Biotechnology Research, 9600 Gudelsky Dr, Rockville, MD 20850, USA

SUPPORTING INFORMATION

Text

Details of the NMR Measurements. The spectra recorded on the different samples are summarized in SI Table S1, with the compositions of the various samples summarized in SI Table S2. Liquid crystalline solutions were prepared as follows: (A) Pf1 samples were obtained by mixing stock solutions of 50 mg/mL Pf1 (http://www.asla-biotech.com) with protein solutions, followed by mild vortexing. All Pf1-related NMR data were collected at 293 K. (B) Bicelle samples were prepared by mixing 1,2-dihexanoyl-sn-glycero-3-phosphocholine (DHPC) with 1,2-dimyristoyl-sn-glycero-3-phosphocholine (DMPC) and cetyl trimethylammonium bromide (CTAB) at a molar ratio [DHPC]:[DMPC]:[CTAB] of 1:3:0.05. The final NMR sample bicelle concentration was 4.5% w/v. All bicelle-related NMR data were acquired at 308 K. (C) PEG samples were prepared by mixing penta-ethylene glycol monododecyl ether (C12E5; Sigma Aldrich), with hexanol at a molar ratio [PEG]:[hexanol] of 3:2.[1] The final PEG concentration in the NMR sample was 5.5% w/v. All PEG-related NMR data were acquired at 301 K. The absence of significant chemical shift changes over the 293-308 K temperature range was used as evidence for the absence of any significant structural change.

Uniformly {^{13}C, ^{15}N}-enriched NMR samples in 95% H_2O, 5% D_2O, 20 mM sodium phosphate buffer, 50 mM NaCl, pH 6.5, and 0.05% sodium azide, were used to record the following spectra: ^{15}N-^{1}H ARTSY for measurement of $^{1}D_{NH}$;[2] HA[HN,HB](CACO)NH for $^{3}J_{H\alpha-H\beta}$;[3] CT-HN(COCA)CB for the sum of $^{1}D_{C\beta H\beta 2}$ and $^{1}D_{C\beta H\beta 3}$. The CT-HN(COCA)CB pulse scheme used is analogous to the scheme of Yamazaki et al.[4] but adapted to have $^{1}H^{\beta}$-coupled $^{13}C^{\beta}$ evolution (SI Figure S1). The ^{15}N-^{1}H ARTSY spectra were recorded at 600 MHz, using time domain matrices consisting of 150* × 1024* complex data points, or acquisition times of 78 ms (t_1, ^{15}N) and 121 ms (t_2, ^{1}H), using 8 scans per free induction decay (FID), and a 2-s interscan delay (total measurement time ca 1.5 h).

HA[HN,HB](CACO)NH spectra were recorded at 600 MHz, with the ^{13}C and ^{15}N carriers at 46 and 118 ppm, respectively. The time domain matrices consisted of 200* × 20* × 1024* complex data points, or acquisition times of 36 ms (t_1, ^{1}H), 10 ms (t_2, ^{15}N) and 85 ms (t_3, ^{1}H), using 8 scans per FID, and a 1.5 s interscan delay (total measurement time *ca* 64 h). The CT-HN(COCA)CB spectra were also recorded at 600 MHz, with the ^{13}C and ^{15}N carriers set at 43 and 122 ppm, respectively. The time domain matrices consisted of 267* × 22* × 1024* complex data points, or acquisition times of 27 ms (t_1, ^{13}C), 11 ms (t_2, ^{15}N) and 136 ms (t_3, ^{1}H), using 4 scans per FID and a 1.5 s interscan delay (total measurement time *ca* 48 h).

Uniformly {^{13}C, ^{15}N}-labeled NMR samples in 99.8% D_2O, 50 mM sodium phosphate buffer, 50 mM sodium chloride, pD 6.5 (uncorrected meter reading), and 0.05% sodium azide, were used to record the following spectra: ^{1}H-^{13}C CT-HSQC for measurement of $^{1}D_{C\alpha H\alpha}$; ^{1}H-^{13}C CT-HSQC lacking $^{13}C'$ and aromatic $^{13}C^{\gamma}$ decoupling for measurement of $^{1}D_{C\beta C\gamma}$ in Phe, Tyr, Asp and Asn; non-CT ^{1}H-^{13}C HSQC spectra for methyl group $^{1}D_{C\beta C\gamma}$ in Val, Ile, and Thr; and ^{1}H-^{13}C HSQC for measurement of $^{1}D_{C\alpha C\beta}$. ^{1}H-^{13}C HSQC spectra were recorded at 900 MHz. For measurement of $^{1}D_{C\alpha C\beta}$, the ^{13}C and ^{15}N carriers were set at 56 and 118 ppm, respectively and the time domain matrices consisted of 1024* × 1024* complex data points, or acquisition times of 106 ms (t_1, ^{13}C) and 103 ms (t_2, ^{1}H), using 4 scans per FID, and a 1.5 s interscan delay (*ca* 2 h measurement time per spectrum). For the ^{1}H-^{13}C CT-HSQC measurement of $^{1}D_{C\alpha H\alpha}$, the ^{13}C and ^{15}N carriers were set at 49 and 118 ppm, respectively and the time domain matrices consisted of 1108* × 1024*

complex data points, or acquisition times of 55.4 ms (t_1, ^{13}C) and 103 ms (t_2, ^{1}H), using 8 scans per FID, and a 1.5 s interscan delay (*ca* 8 h total measurement time). For measurement of $^{1}D_{C\beta C\gamma}$ in Phe, Tyr, Asp and Asn, the ^{13}C and ^{15}N carriers were set at 40 and 118 ppm, respectively. The time domain matrix consisted of 1101* × 1024* complex data points, or acquisition times of 55 ms (t_1, ^{13}C) and 103 ms (t_2, ^{1}H), and using 4 scans per FID (*ca* 4 h total measurement time). For non-CT ^{1}H-^{13}C HSQC spectra, the ^{13}C and ^{15}N carriers were set at 20 and 118 ppm, respectively. The time domain matrices consisted of 650* × 1024* complex data points, or acquisition times of 84.5 ms (t_1, ^{13}C) and 206 ms (t_2, ^{1}H), using 4 scans per FID, and a 1.5 s interscan delay (*ca* 2.5 h total measurement time).

Uniformly {^{13}C,^{15}N}-enriched, fractionally (75%) deuterated NMR samples were in 99.8% D_2O, 50 mM sodium phosphate buffer, 50 mM NaCl, pD 6.5, 0.05% sodium azide, and were used to record DEPT-filtered ^{1}H-^{13}C CT-HSQC (SI Figure S2) spectra for measurement of individual $^{1}D_{C\beta H\beta 2}$ and $^{1}D_{C\beta H\beta 3}$ values, as well as $^{1}D_{C\alpha H\alpha}$ to calibrate alignment strength. The DEPT-filtered ^{1}H-^{13}C CT-HSQC spectra were recorded at 900 MHz, with the ^{13}C and ^{15}N carriers set at 49 and 118 ppm, respectively. The time domain matrices consisted of 824* × 1024* complex data points, or acquisition times of 48 ms (t_1, ^{13}C) and 103 ms (t_2, ^{1}H), using 8 scans per free induction decay (FID), and a 1.5 s interscan delay (*ca* 6 h total measurement time).

Uniformly {^{2}H,^{13}C,^{15}N}-enriched NMR samples were in 95% H_2O, 5% D_2O, 50 mM sodium phosphate buffer, 50 mM NaCl, pH 6.5, 0.05% sodium azide, and were used to record ^{1}H-^{15}N-HSQC (^{15}N-^{1}H ARTSY) spectra for $^{1}D_{NH}$ (for alignment strength calibration) and 3D HN(CO)CA spectra with a long $^{13}C^{\alpha}$ acquisition time (106 ms) for measurement of $^{1}D_{C\alpha C\beta}$, both at 600 MHz. The 3D HN(CO)CA time domain matrices consisted of 40* × 225* × 1024* complex data points, or acquisition times of 28 ms (t_1, ^{15}N), 106 ms (t_2, ^{13}C) and 136 ms (t_3, ^{1}H), using 4 scans per free induction decay (FID), and a 1.5 s interscan delay (*ca* 72 h total measurement time).

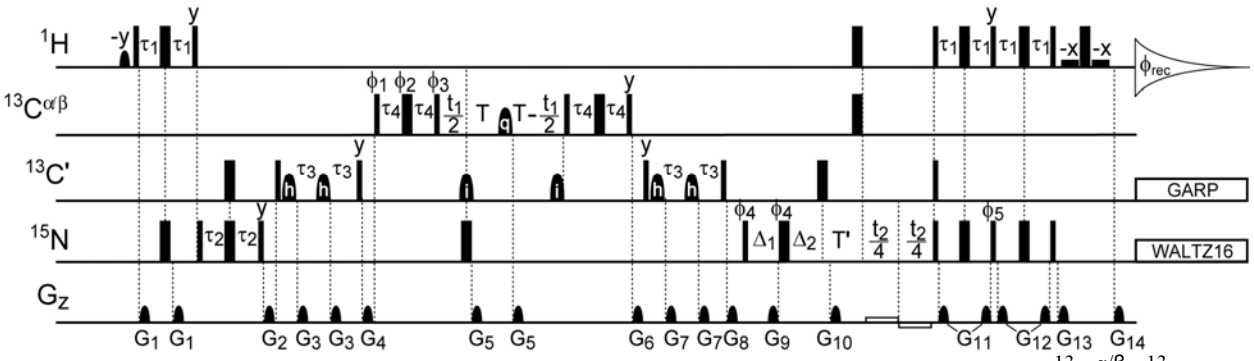

Figure S1. Pulse scheme of the CT-HN(COCA)CB experiment. The carriers of $^{13}C^{\alpha/\beta}$, $^{13}C'$ and ^{15}N are at 43, 176 and 122 ppm Pulse durations should scale inversely with the magnetic field strength, and at 150.90 MHz ^{13}C (600.1 MHz ^{1}H) frequency the following settings were used: Rectangular low-power and SINC-shaped ^{1}H pulses are applied using $\gamma_H B_1$ = 208 and 278 Hz (at its midpoint), respectively. The RF strength of ^{13}C 90°/180° rectangular pulses is 5.2/11.7 kHz. The $^{13}C'$ selective Hyperbolic-Secant [5] and IBURP2 [6] pulses are marked with h and i, respectively, and have a duration of 600 and 400 µs (centered at 116 and 160 ppm); The $^{13}C^{\alpha/\beta}$ selective Q3 pulses are marked with q, and have a duration of 220 µs. ^{13}C GARP / ^{15}N WALTZ16 decoupling [7] during ^{1}H acquisition is applied at an RF field strength of 1.8/1.2 kHz. Unless specified, all pulse phases are *x*. Phase cycling: $\phi_1 = y,-y$; $\phi_2 = x,-x$; $\phi_3 = x,-x$; $\phi_4 = y,y,-y,-y$; $\phi_5 = y$; and $\phi_{rec} = x,-x,-x,x$. Delay durations: $\tau_1 = 1/(4J_{HN}) \approx 2.7$ ms; $\tau_2 = 1/(4J_{NC'}) \approx 12.5$ ms; $\tau_3 \approx 4$ ms; $\tau_4 = 1/(4J_{C\alpha C\beta}) \approx 7.2$ ms; T = 14.1 ms; T' = 12.5 ms; $\Delta_1 = \max(0, T' - 0.5 \times t_2)$; $\Delta_2 = \max(0, 0.5 \times t_2 - T')$. Gradient pulses $G_{1,\ldots,14}$ (z-axis) have durations of 1800, 500, 2000, 500, 137, 1000, 2400, 500, 500, 500, 250, 800, 200 and 301 µs, and strengths of 3.5, 25.9, 4.2, 27.3, 28.7, 34.3, 4.9, 31.5, 37.8, -44.8, 21.0, 37.1, 41.3, and 41.3 G/cm. The weak (0.77 G/cm) bipolar gradient applied during the second half of the t_2 evolution period serves to prevent radiation damping of the inverted H_2O signal. Quadrature detection in the t_1 dimension is achieved by increasing ϕ_1, ϕ_2, ϕ_3 in the regular States-TPPI manner; quadrature in the t_2 dimension is obtained by the Rance-Kay method, inverting G_9/G_{10} and ϕ_5.

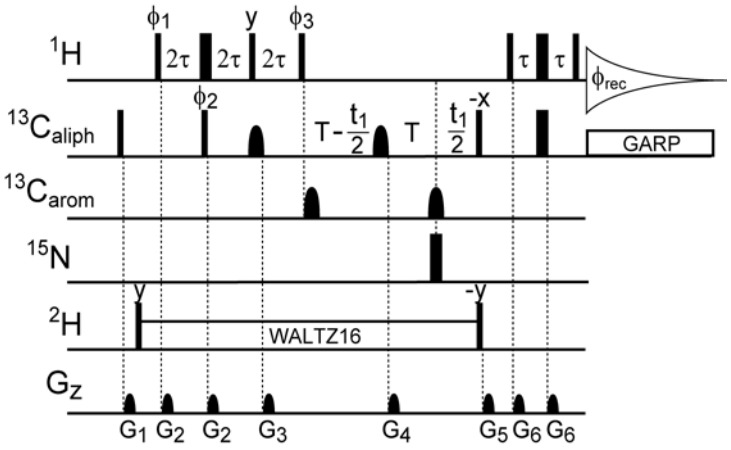

Figure S2. Pulse scheme of the DEPT-filtered ^{1}H-^{13}C CT-HSQC experiment. The carrier of $^{13}C_{aliph}$ is at 49 ppm. Narrow and wide bars indicate non-selective 90° and 180° pulses, respectively. Pulse durations should scale inversely with the magnetic field strength, and at 226.37 MHz ^{13}C frequency the following values were used: The $^{13}C_{aliph}$ and $^{13}C_{arom}$ shaped pulses are Hyperbolic-Secant and IBURP2, with durations of 550 and 300 μs (centered at 20 and 151 ppm), respectively. ^{13}C GARP decoupling during acquisition is applied at an RF field strength of 3.8 kHz. ^{2}H decoupling is applied using the WALTZ-16 scheme with an RF field strength of 833 Hz. Unless specified, all pulse phases are *x*. Phase cycling: ϕ_1 = *x*,*x*,-*x*,-*x*; ϕ_2 = *x*,*x*,*x*,*x*,-*x*,-*x*,-*x*,-*x*; ϕ_3 = *x*,-*x*; and ϕ_{rec} = *x*,*x*,-*x*,-*x*,-*x*,-*x*,*x*,*x*. Delay durations: $\tau = 1/(4J_{CH}) \approx 1.8$ ms; T = 24.2 ms. Gradient pulses $G_{1,\ldots,6}$ (z-axis) have durations of 1.5, 1.0, 1.0, 1.0, 0.6 and 1.0 ms, and strengths of 23.8, 28.7, 40.6, 11.9, -33.6, and 21.7 G/cm. Quadrature detection in the t_1 dimension is achieved by increasing ϕ_2 in the regular States-TPPI manner.

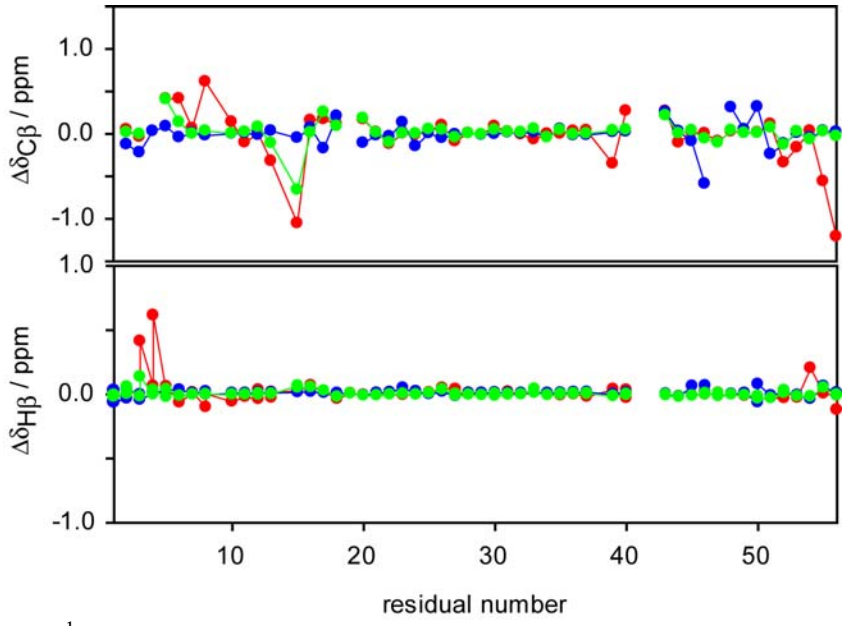

Figure S3. $^{13}C_\beta$ and $^{1}H_\beta$ chemical shift difference from Table S3 and S4. $\Delta\delta$ is the chemical shift difference between wild-type GB3 and mutant. Red, blue and green represent mutants K4A/K19E/V42E-CHis$_6$, K19A/V42E/D47K and K4A/K19E/V42E respectively.

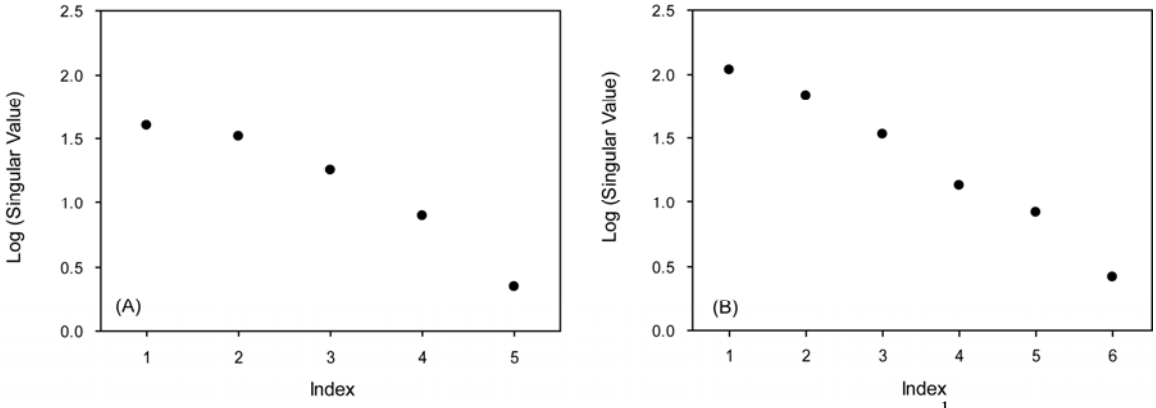

Figure S4. Singular value decomposition of (A) alignment tensors, (B) $^{1}D_{NH}$ RDCs for six different alignment conditions (three different media, plus three mutants).

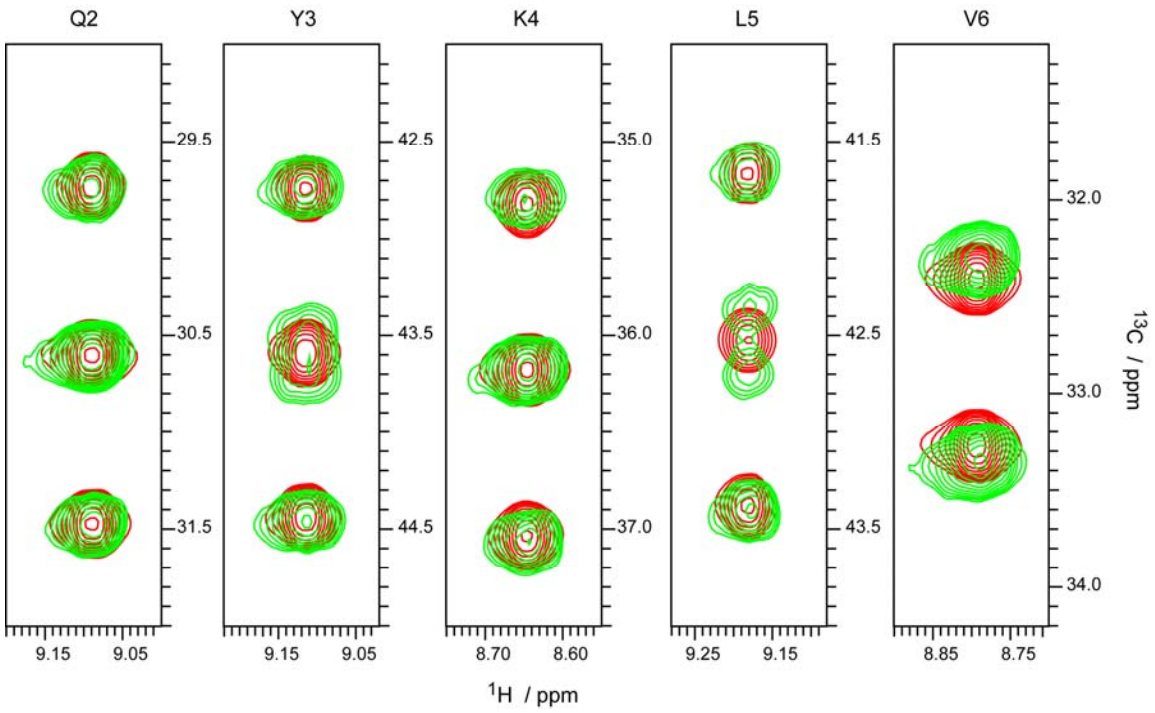

Figure S5. Strips from the 3D CT-HN(COCA)CB spectrum, used for deriving the sum of $^{1}D_{C\beta H\beta 2}$ and $^{1}D_{C\beta H\beta 3}$. Red contours represent the isotropic wild-type GB3 spectrum; green contours are strips from the same GB3 sample aligned with 4.5% bicelles. The multiplets shown correspond to the ^{1}H-coupled $^{13}C^{\beta}$ resonances of residues Q2, Y3, K4, L5, and V6.

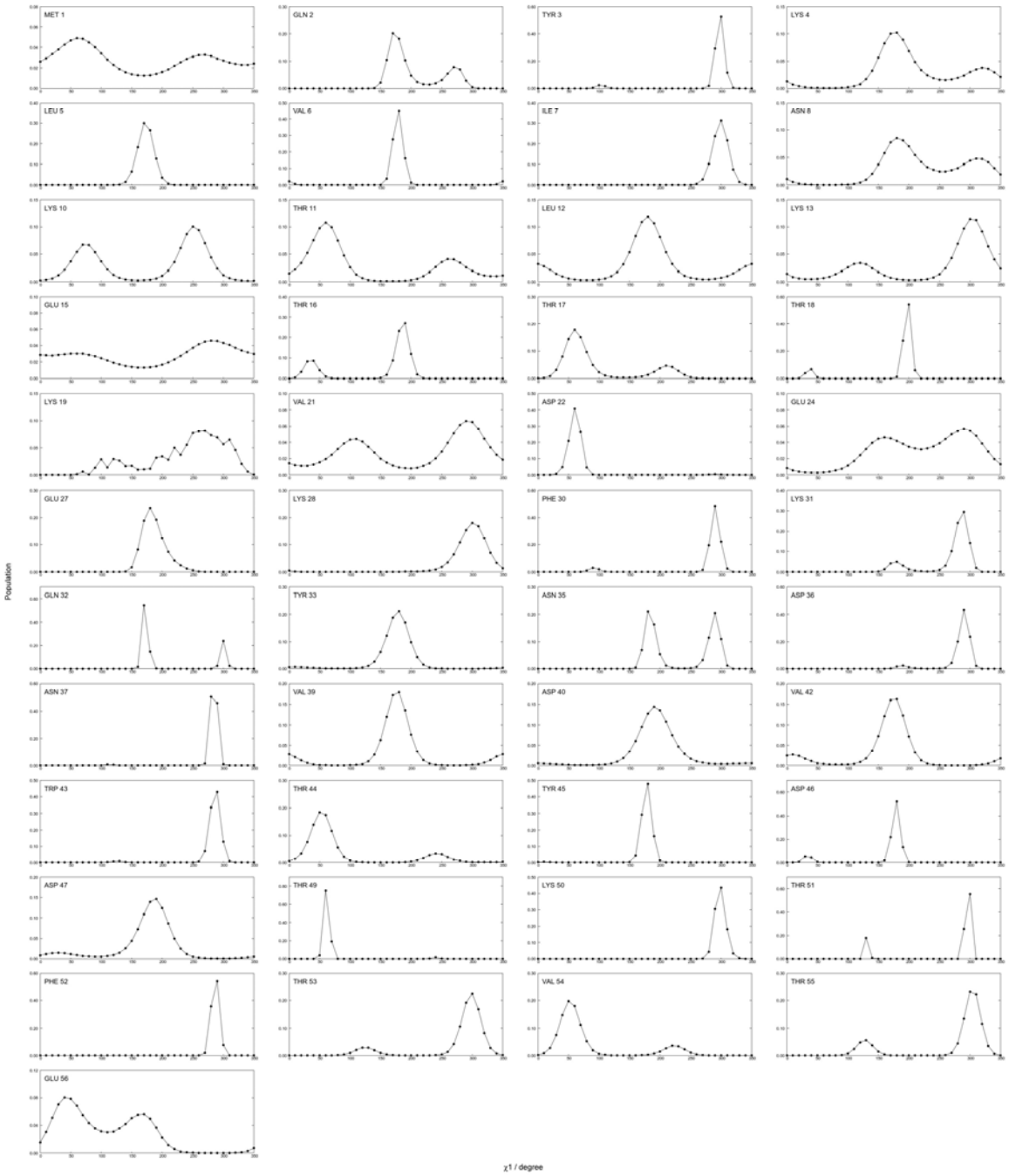

Figure S6. Distributions of χ_1 torsion angles for all residues in GB3, derived from RDC data. (see also Figure 4, main text)

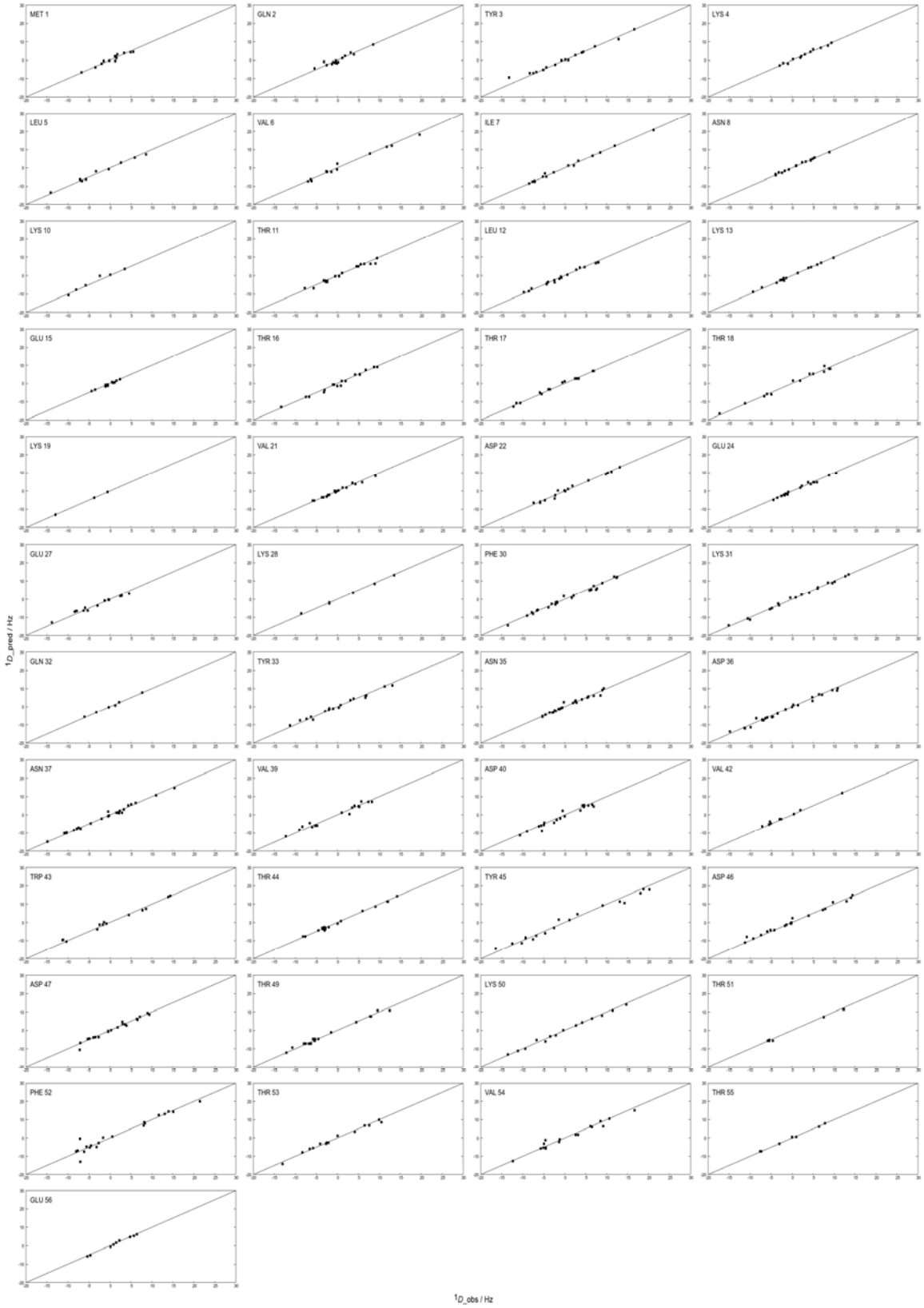

Figure S7: The correlations between observed and predicted RDCs from the result of the χ_1 ensemble VW-Fit program in Figure S6.

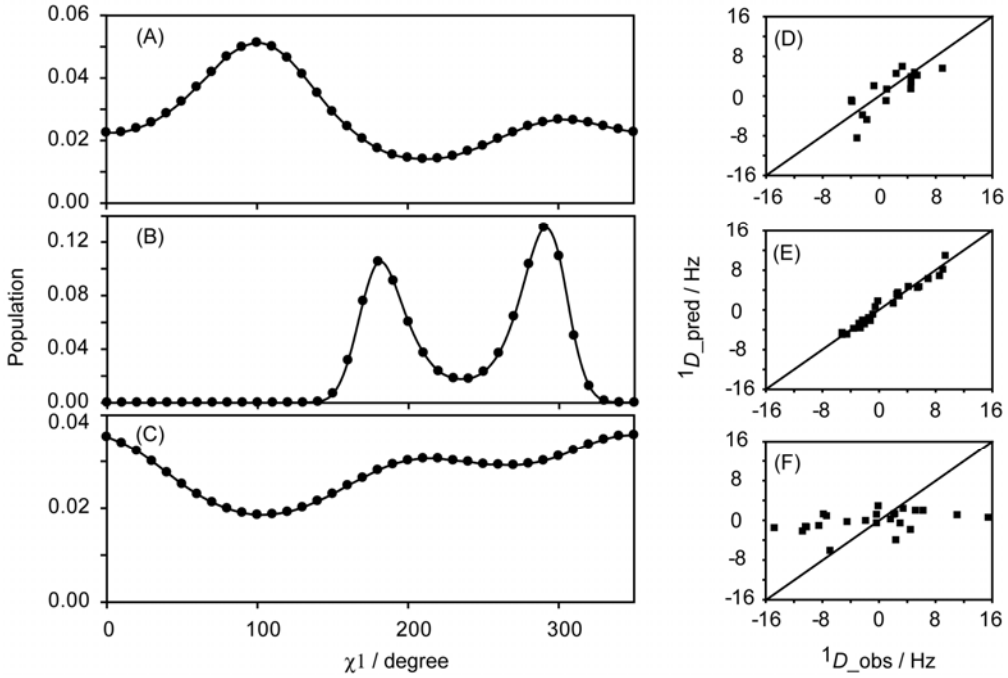

Figure S8. Distributions of χ_1 torsion angles for the three Asn residues, (A) Asn8, (B) Asn35, (C) Asn37, in GB3 with reversed $H^{\beta 2}$ and $H^{\beta 3}$ stereospecific assignments. The correlations between observed and predicted RDCs for these residues are shown in panels (D) Asn8, (E) Asn35, (F) Asn37. The results of correct stereospecific assignments are shown in Figure 4, main text.

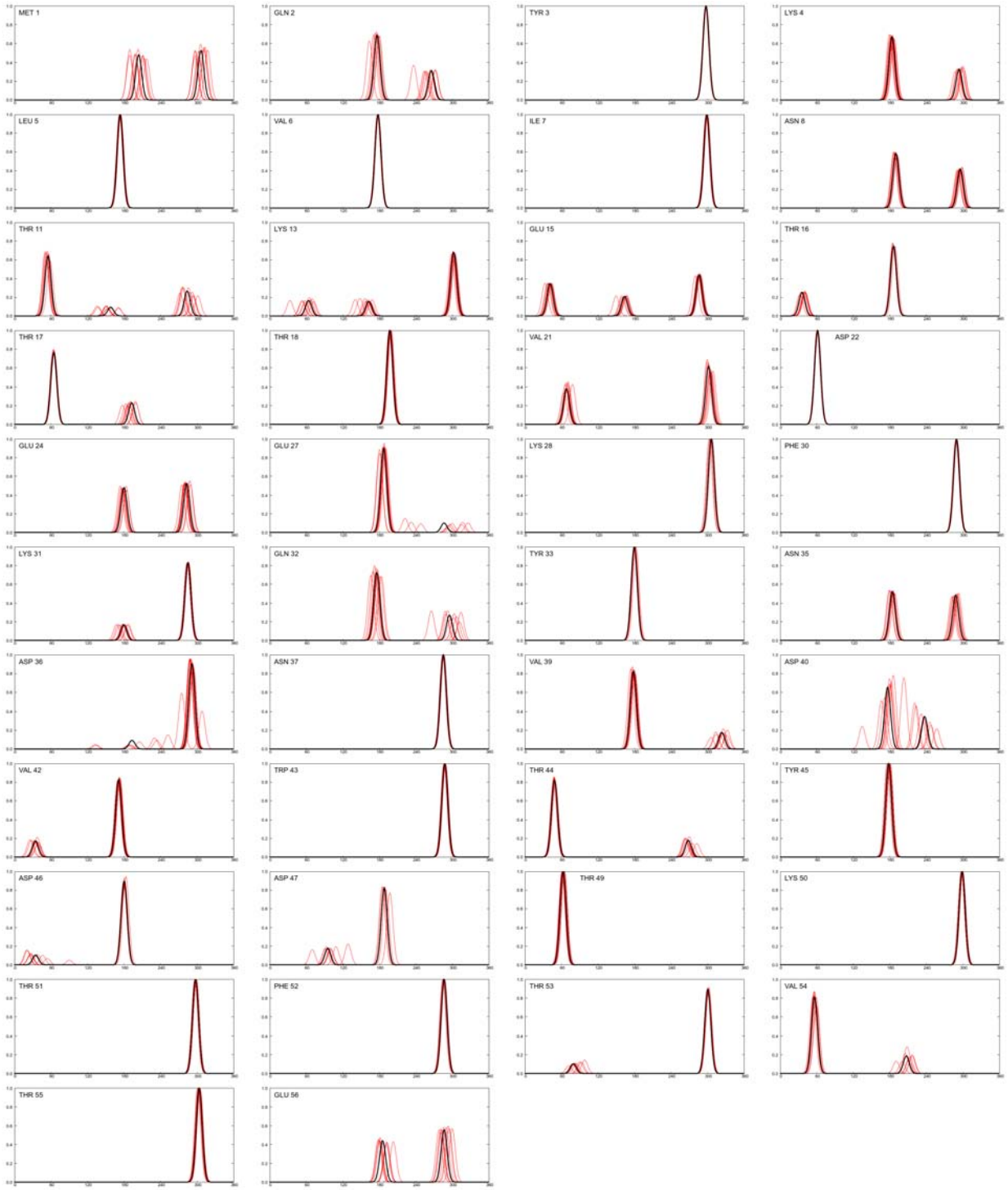

Figure S9. Effect of uncertainty in the structure and sidechain RDC data on χ_1 distributions obtained by Monte Carlo rotamer analysis for all residues.

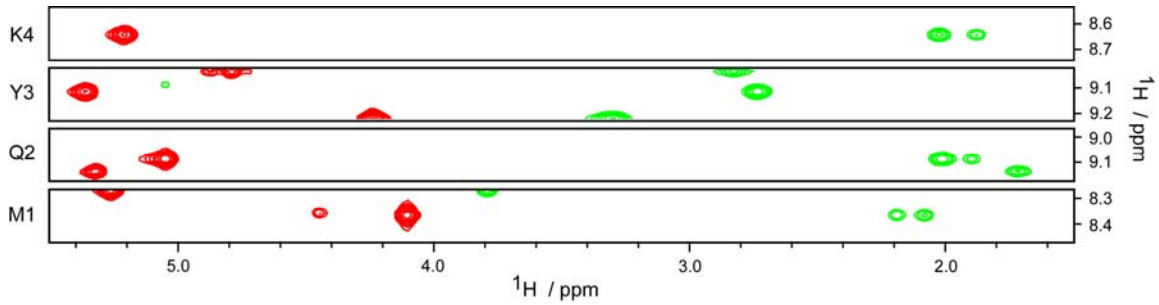

Figure S10. Aliphatic region from strips taken from the 3D HA[HN,HB](CACO)NH spectrum, used for measuring $^3J_{H\alpha H\beta}$.[3] The H^{α} diagonal peaks are in red; H^{α}-H^{β} cross peaks have opposite signs and are shown in green.

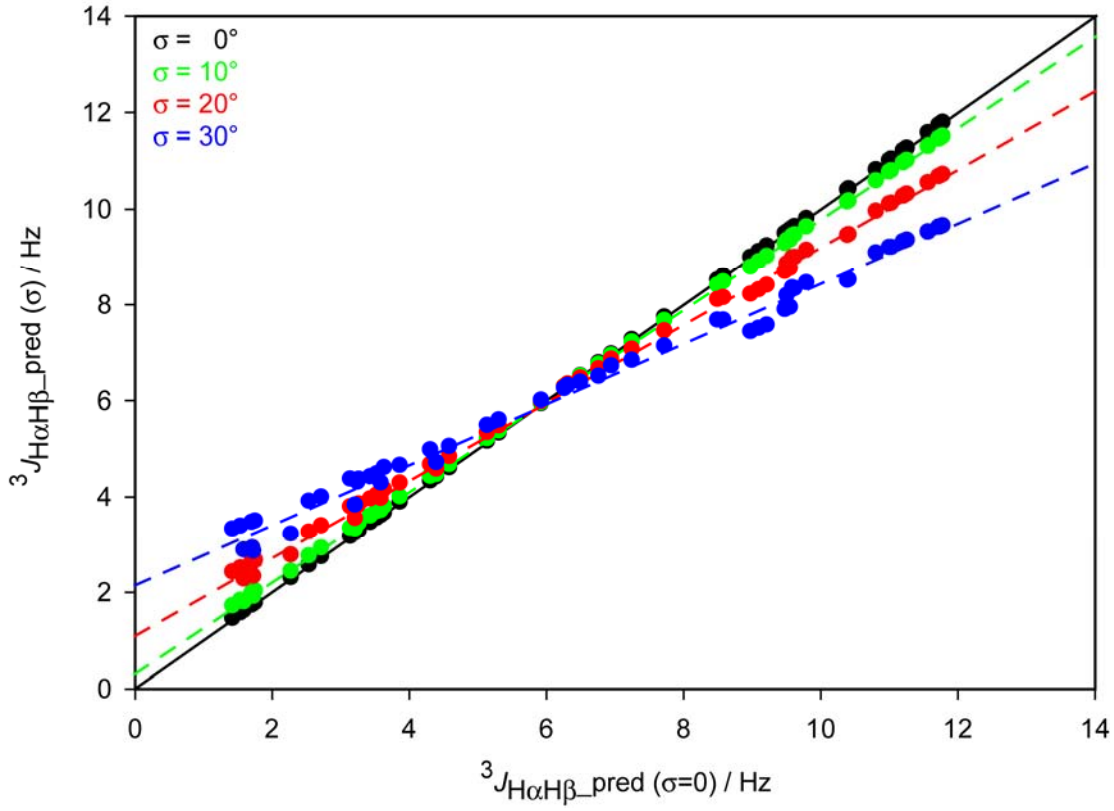

Figure S11. Correlations between predicted $^3J_{H\alpha H\beta}(\sigma=0)$ and $^3J_{H\alpha H\beta}(\sigma)$ couplings. $^3J_{H\alpha H\beta}$ are generated by the substituent-specific Karplus equations of Haasnoot et al. for the residue types and χ_1 angles reported in main text Table 1, using the Karplus equations of Table S9. For each rotamer, the motion-modified (cf eq 4) $^3J_{H\alpha H\beta}$ is predicted prior to calculating the displayed, weighted sum. σ is the standard deviation to the χ_1 angles.

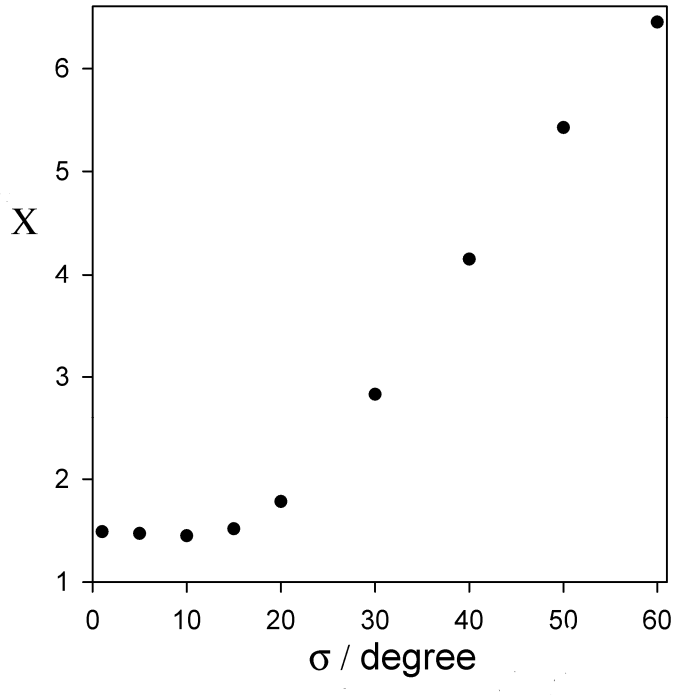

Figure S12. Value for the normalized Chi (X) value as a function of the standard deviation, σ, of the Gaussian rotamer distribution obtained for the best fit between the observed and predicted RDC values when using the discrete-rotamer model, with the model selection parameters of Table 1, as a function of the width of the Gaussian distribution used for each rotamer. For fits involving multiple rotamers, the same Gaussian width was assumed for each fitted rotamer. The reported average X value represents the average over all residues reported in Table 1, main text.

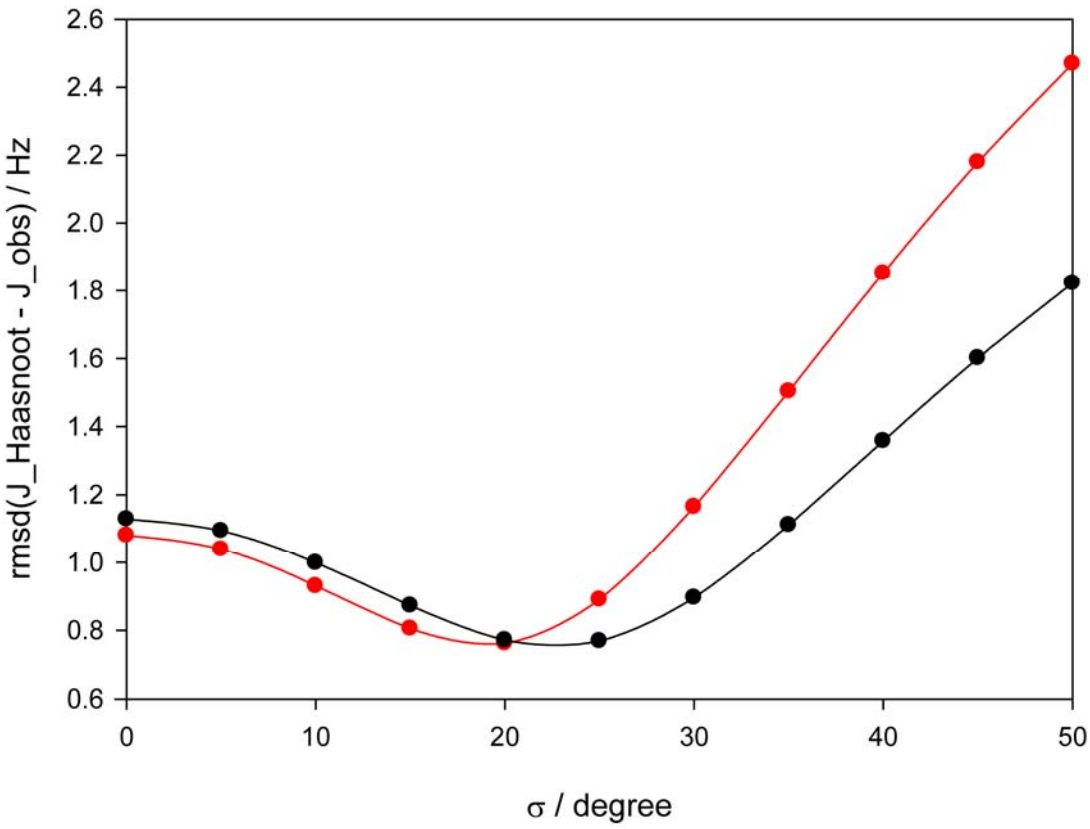

Figure S13. Root-mean-square difference between the sigma-corrected Haasnoot-Karplus $^{3}J_{H\alpha H\beta}$ predictions and observed values, as a function of the amplitude of the Gaussian fluctuations. (black) All residues for which $^{3}J_{H\alpha H\beta}$ values were available are included in the rmsd calculation, regardless of the number of rotamers observed and listed in Table 1, main text. (red) Only residues for which a single rotamer was selected in Table 1 were used for the rmsd calculation.

Table S1. Summary of NMR spectra recorded for each of the different samples

Sample	Spectra	RDC type	^{1}H frequency / MHz
Sample I: {^{13}C, ^{15}N} in H_2O [a]	ARTSY	$^1D_{NH}$	600
	CT-HN(COCA)CB	$^1D_{C\beta H\beta 2} + {}^1D_{C\beta H\beta 3}$	
Sample II: {^{13}C, ^{15}N} in D_2O	^{1}H-^{13}C HSQC	$^1D_{C\alpha C\beta}$	900
	^{1}H-^{13}C CT-HSQC	$^1D_{C\alpha H\alpha}$	
	^{1}H-^{13}C CT-HSQC (aromatic) non-CT ^{1}H-^{13}C HSQC (methyl)	$^1D_{C\beta C\gamma}$	
Sample III: 75% deuterated {^{13}C, ^{15}N} in D_2O	DEPT-filtered ^{1}H-^{13}C CT-HSQC	$^1D_{C\alpha H\alpha}$, $^1D_{C\beta H\beta 2}$, $^1D_{C\beta H\beta 3}$	900
Sample IV: {^{2}H, ^{13}C, ^{15}N} in H_2O	ARTSY	$^1D_{NH}$	600
	HN(CO)CA	$^1D_{C\alpha C\beta}$	

[a] Sample I: uniformly {^{13}C, ^{15}N}-enriched NMR samples in 95% H_2O, 5% D_2O, 20 mM sodium phosphate buffer, 50 mM NaCl, pH 6.5, and 0.05% sodium azide; Sample II: uniformly {^{13}C, ^{15}N}-enriched NMR samples in 99.8% D_2O, 50 mM sodium phosphate buffer, 50 mM sodium chloride, pD 6.5 (uncorrected meter reading), and 0.05% sodium azide; Sample III: uniformly {^{13}C,^{15}N}-enriched, fractionally (75%) deuterated NMR samples were in 99.8% D_2O, 50 mM sodium phosphate buffer, 50 mM NaCl, pD 6.5, and 0.05% sodium azide; Sample IV: uniformly {^{2}H,^{13}C,^{15}N}-enriched NMR samples were in 95% H_2O, 5% D_2O, 50 mM sodium phosphate buffer, 50 mM NaCl, pH 6.5, and 0.05% sodium azide.

Table S2. Compositions of samples used for NMR experiments

Sample		Sample I: {^{13}C, ^{15}N} in H_2O [a]		Sample II: {^{13}C, ^{15}N} in D_2O		Sample III: 75% deuterated {^{13}C, ^{15}N} in D_2O		Sample IV: {^{2}H, ^{13}C, ^{15}N} in H_2O	
		C_p / mM [b]	LX concentr.(mg/mL)	C_p / mM	LX concentr. (mg/mL)	C_p / mM	LX concentr. (mg/mL)	C_p / mM	LX concentr. (mg/mL)
Wild-type GB3	isotropic [e]	2.5		1.7		3.2		0.5	
	Bicelle	0.5	45	0.7	45	1.5	45	0.5	45
	PEG	0.5	55	1.4	55	0.7	55	0.5	55
	Pf1	1.2	7	1.6	5	1.3	7	0.5	9
Mutant 1 (K4A/K19E/V42E-$CHis_6$)	isotropic	0.9		0.9		1.1			
	Pf1	0.7	12	0.6	8	0.9	6		
Mutant 2 (K19A/V42E/D47K)	isotropic	1.3		0.9		2.2			
	Pf1	1.1	10	0.5	7	1.2	7		
Mutant 3 (K4A/K19E/V42E)	isotropic	2.0		1.2		1.2			
	Pf1	1.0	33	1.0	21	0.4	20		

[a] Samples are the same as the ones in Table S1.
[b] Protein concentration.
[c] All isotropic and Pf1 spectra were recorded at 293K; bicelle and PEG spectra were obtained at 308 and 301 K, respectively.

Table S3. $^{13}C^{\beta}$ Chemical shift for GB3 and three mutants

Res#	AA type	$\delta_{C\beta}$ / ppm [a]				$\Delta\delta_{C\beta}$ / ppm [b]		
		GB3	Mutant 1 [c]	Mutant 2	Mutant 3	Mutant 1	Mutant 2	Mutant 3
1	MET		32.88	32.84	32.94			
2	GLN	30.60	30.65	30.48	30.62	0.05	-0.13	0.01
3	TYR	43.59	43.55	43.37	43.58	-0.04	-0.22	-0.01
4	LYS	36.18	22.85	36.21	22.82	- [d]	0.03	-
5	LEU	42.52	42.93	42.61	42.93	0.41	0.09	0.41
6	VAL	32.84	33.25	32.80	32.98	0.41	-0.04	0.14
7	ILE	39.25	39.31	39.25	39.24	0.06	0.01	0.00
8	ASN	37.79	38.40	37.77	37.82	0.61	-0.02	0.03
10	LYS	32.62	32.76	32.62	32.63	0.14	0.00	0.00
11	THR	69.87	69.76	69.87	69.89	-0.11	0.01	0.02
12	LEU	43.37	43.38	43.36	43.45	0.01	-0.01	0.08
13	LYS	34.74	34.42	34.78	34.63	-0.32	0.03	-0.11
15	GLU	34.00	32.94	33.95	33.34	-1.06	-0.05	-0.66
16	THR	69.52	69.68	69.59	69.54	0.16	0.07	0.01
17	THR	73.33	73.50	73.15	73.58	0.17	-0.17	0.26
18	THR	69.99	70.10	70.20	70.08	0.11	0.21	0.09
19	LYS	33.69	30.53	19.91	30.55	-	-	-
20	ALA	23.79	23.96	23.68	23.97	0.17	-0.11	0.18
21	VAL	32.04	32.06	32.02	32.05	0.02	-0.02	0.01
22	ASP	42.38	42.26	42.35	42.28	-0.12	-0.03	-0.10
23	ALA	17.61	17.61	17.75	17.62	0.00	0.13	0.00
24	GLU	29.05	29.04	28.90	29.05	-0.01	-0.15	0.00
25	THR	67.89	67.94	67.90	67.94	0.04	0.00	0.05
26	ALA	17.55	17.65	17.50	17.60	0.10	-0.05	0.05
27	GLU	29.18	29.08	29.17	29.13	-0.09	-0.01	-0.05
28	LYS	32.41	32.42	32.42	32.42	0.01	0.00	0.00
29	ALA	17.40	17.39	17.39	17.39	-0.01	-0.01	-0.01
30	PHE	37.63	37.72	37.62	37.67	0.09	0.00	0.05
31	LYS	31.57	31.59	31.58	31.59	0.02	0.02	0.02
32	GLN	28.25	28.24	28.25	28.26	-0.01	0.01	0.02
33	TYR	38.60	38.53	38.61	38.65	-0.07	0.02	0.06
34	ALA	17.86	17.86	17.82	17.82	0.00	-0.04	-0.04
35	ASN	38.78	38.78	38.84	38.83	0.00	0.05	0.04
36	ASP	40.03	40.06	40.01	40.02	0.03	-0.02	-0.01
37	ASN	40.10	40.14	40.09	40.11	0.04	-0.02	0.00
39	VAL	33.39	33.03	33.41	33.42	-0.35	0.02	0.04
40	ASP	42.99	43.26	43.01	43.04	0.27	0.02	0.05
42	VAL	33.57	31.73	31.57	31.55	-	-	-
43	TRP	30.27	30.54	30.53	30.48	0.27	0.26	0.21
44	THR	72.37	72.26	72.39	72.37	-0.11	0.03	0.00
45	TYR	41.58	41.59	41.49	41.61	0.02	-0.09	0.04
46	ASP	43.14	43.14	42.55	43.08	0.00	-0.59	-0.06
47	ASP	42.18	42.09	32.49	42.07	-0.09	-	-0.11
48	ALA	18.30	18.33	18.61	18.35	0.03	0.31	0.04
49	THR	70.19	70.20	70.24	70.19	0.01	0.05	0.01
50	LYS	29.36	29.38	29.68	29.37	0.02	0.32	0.01
51	THR	72.11	72.22	71.87	72.18	0.11	-0.24	0.07

52	PHE	42.64	42.30	42.52	42.51	-0.34	-0.12	-0.13
53	THR	70.99	70.83	71.00	71.02	-0.16	0.01	0.03
54	VAL	32.45	32.48	32.40	32.38	0.03	-0.05	-0.07
55	THR	70.81	70.25	70.84	70.84	-0.56	0.03	0.03
56 [e]	GLU	32.04	30.83	32.06	32.01	-1.21	0.02	-0.03

[a] $\delta_{C\beta}$ as measured from CT-HN(COCA)CB spectra.
[b] $\Delta\delta_{C\beta}$ is the $^{13}C_\beta$ chemical shift difference between wild-type GB3 and mutant. RDCs from residues for which $|\Delta\delta_{C\beta}| > 0.2$ ppm are excluded from the analysis.
[c] Mutants 1-3 represent K4A/K19E/V42E-CHis$_6$, K19A/V42E/D47K and K4A/K19E/V42E respectively.
[d] – indicates the site of mutation.
[e] $\delta_{C\beta}$ as derived from the DEPT-filtered ^{1}H-^{13}C CT-HSQC spectrum.

Table S4. $^{1}H^{\beta}$ Chemical shift for GB3 and three mutants

Res#	AA type	proton	$\delta_{H\beta}$ / ppm [a]				$\Delta\delta_{H\beta}$ / ppm [b]		
			GB3	Mutant 1 [c]	Mutant 2	Mutant 3	Mutant 1	Mutant 2	Mutant 3
1	MET	Hβ2	2.20	2.19	2.23	2.19	-0.01	0.03	-0.01
1	MET	Hβ3	2.08	2.07	2.02	2.07	-0.02	-0.06	-0.02
2	GLN	Hβ2	1.88	1.94	1.93	1.94	0.05	0.05	0.06
2	GLN	Hβ3	2.00	2.00	1.96	2.00	0.00	-0.03	0.00
3	TYR	Hβ2		2.73	2.78	2.73			
3	TYR	Hβ3	3.43	3.40	3.42	3.41	-0.03	0.00	-0.02
4	LYS	Hβ2	1.86	-	1.88	-	-	0.01	-
4	LYS	Hβ3	2.00	- [d]	2.01	-	-	0.01	-
5	LEU	Hβ2	-1.21	-1.15	-1.17	-1.17	0.06	0.03	0.04
5	LEU	Hβ3	0.74	0.75	0.76	0.72	0.01	0.02	-0.02
6	VAL	Hβ	2.05	1.99	2.09	2.04	-0.07	0.03	-0.01
7	ILE	Hβ	1.54	1.55	1.54	1.53	0.01	0.01	0.00
8	ASN	Hβ2	2.50	2.50	2.49	2.50	0.00	0.00	0.00
8	ASN	Hβ3	2.94	2.84	2.96	2.94	-0.10	0.02	0.00
10	LYS	Hβ# [e]	1.79	1.73	1.79	1.78	-0.06	0.01	0.00
11	THR	Hβ	4.17	4.15	4.18	4.17	-0.02	0.01	0.00
12	LEU	Hβ2	1.36	1.39	1.36	1.36	0.03	0.01	0.00
12	LEU	Hβ3	1.56	1.52	1.57	1.56	-0.04	0.01	-0.01
13	LYS	Hβ2	1.70	1.72	1.71	1.70	0.02	0.01	0.00
13	LYS	Hβ3	1.85	1.82	1.86	1.85	-0.03	0.01	0.00
15	GLU	Hβ2 [f]	1.89	1.93	1.91	1.94	0.03	0.01	0.05
15	GLU	Hβ3 [f]	2.01	2.03	2.02	2.07	0.03	0.02	0.07
16	THR	Hβ	3.92	3.99	3.94	3.97	0.07	0.02	0.05
17	THR	Hβ	4.28	4.30	4.29	4.30	0.02	0.01	0.03
18	THR	Hβ	3.77	3.74	3.78	3.75	-0.04	0.01	-0.02
19	LYS	Hβ#	1.69	-	-	-	-	-	-
20	ALA	Hβ#	1.31	1.31	1.30	1.30	-0.01	-0.01	-0.01
21	VAL	Hβ	2.17	2.16	2.18	2.16	-0.01	0.01	-0.01
22	ASP	Hβ2	3.08	3.08		3.07	0.00		0.00
23	ALA	Hβ#	1.15	1.15	1.20	1.15	-0.01	0.05	0.00
24	GLU	Hβ2	1.95	1.95	1.97	1.95	0.00	0.02	0.00
24	GLU	Hβ3	1.78	1.79	1.79	1.78	0.00	0.00	0.00
25	THR	Hβ	4.00	4.01	4.00	4.01	0.01	0.00	0.01
26	ALA	Hβ#	0.47	0.51	0.49	0.50	0.05	0.02	0.04
27	GLU	Hβ2	1.90	1.91	1.89	1.89	0.01	-0.02	-0.01
27	GLU	Hβ3	1.82						
28	LYS	Hβ#	1.72	1.72	1.73	1.71	0.00	0.01	0.00
29	ALA	Hβ#	1.18	1.17	1.18	1.17	-0.01	0.01	-0.01
30	PHE	Hβ2	2.83	2.81	2.84	2.81	-0.01	0.01	-0.01
30	PHE	Hβ3	3.33	3.34	3.34	3.33	0.01	0.01	0.00
31	LYS	Hβ2	1.59	1.61	1.59	1.59	0.02	0.00	0.00
31	LYS	Hβ3	1.49	1.49	1.50	1.49	0.00	0.01	0.00
32	GLN	Hβ#	2.18	2.18	2.19	2.18	0.00	0.01	0.00
33	TYR	Hβ2	3.28	3.29	3.30	3.29	0.01	0.02	0.01
33	TYR	Hβ3	3.31	3.33	3.32		0.01	0.01	
34	ALA	Hβ#	1.81	1.80	1.81	1.80	0.00	0.01	-0.01
35	ASN	Hβ2	2.95	2.94	2.96	2.95	-0.01	0.01	0.00

35	ASN	Hβ3	2.90	2.91	2.91	2.89	0.01	0.01	0.00
36	ASP	Hβ2	2.71	2.71	2.73	2.72	0.00	0.01	0.01
36	ASP	Hβ3	2.54	2.55	2.55	2.54	0.01	0.01	0.00
37	ASN	Hβ2	2.06	2.04	2.08	2.07	-0.02	0.02	0.01
37	ASN	Hβ3	2.68	2.67	2.69	2.68	-0.01	0.01	0.00
39	VAL	Hβ	1.74	1.78	1.74	1.72	0.04	0.00	-0.02
40	ASP	Hβ2	2.55	2.59	2.57	2.55	0.03	0.01	0.00
40	ASP	Hβ3	2.74	2.71	2.74	2.73	-0.03	0.01	-0.01
42	VAL	Hβ	1.94	-	-	-	-	-	-
43	TRP	Hβ2	3.14		3.14	3.13		0.00	-0.01
43	TRP	Hβ3	3.33	3.32	3.33	3.33	0.00	0.00	0.00
44	THR	Hβ	4.26	4.24	4.24	4.24	-0.02	-0.02	-0.02
45	TYR	Hβ2	2.87	2.86		2.86	-0.01		-0.01
45	TYR	Hβ3	2.48		2.54			0.06	
46	ASP	Hβ2	2.24	2.24	2.26	2.24	0.00	0.02	0.00
46	ASP	Hβ3	2.57	2.58	2.64	2.58	0.01	0.07	0.01
47	ASP	Hβ2	2.82	2.81	-	2.80	-0.01	-	-0.02
47	ASP	Hβ3	2.49	2.50	-	2.50	0.01	-	0.01
48	ALA	Hβ#	1.46	1.46	1.47	1.46	0.00	0.00	0.00
49	THR	Hβ	4.39	4.38	4.40	4.38	-0.01	0.01	-0.01
50	LYS	Hβ2	2.07	2.03	2.15	2.04	-0.04	0.08	-0.03
50	LYS	Hβ3	2.00	1.98	1.94	1.99	-0.03	-0.06	-0.02
51	THR	Hβ	3.75	3.72	3.74	3.72	-0.03	-0.01	-0.03
52	PHE	Hβ2	3.25	3.27	3.26	3.28	0.02	0.01	0.03
52	PHE	Hβ3	3.20	3.17	3.22	3.21	-0.03	0.02	0.01
53	THR	Hβ	3.80	3.77	3.79	3.78	-0.03	-0.01	-0.02
54	VAL	Hβ	-0.40	-0.19	-0.43	-0.41	0.20	-0.04	-0.02
55	THR	Hβ	3.79	3.79	3.85	3.84	0.00	0.06	0.05
56	GLU	Hβ2	1.93	1.91	1.93	1.92	-0.01	0.00	-0.01
56	GLU	Hβ3	2.13	2.01	2.14	2.13	-0.12	0.01	0.00

[a] $\delta_{H\beta}$ are measured from the DEPT-filtered ^{1}H-^{13}C CT-HSQC spectrum, not corrected for ^{2}H-isotope shift effects

[b] $\Delta\delta_{H\beta}$ is the $^{1}H_{\beta}$ chemical shift difference between wild-type GB3 and mutant. RDCs from residues for which $|\Delta\delta_{H\beta}| > 0.1$ ppm are excluded from the analysis.

[c] Mutants 1-3 represent K4A/K19E/V42E-CHis$_6$, K19A/V42E/D47K and K4A/K19E/V42E respectively.

[d] – indicates the site of mutation.

[e] # represents the two equivalent protons attached to C^{β}.

[f] ambiguous stereospecific assignment.

Table S5. C^{β}-related ^{1}D couplings[a] and their sums (Hz)

bicelle[a]

Res#	AA type		$^{1}D_{C\beta C\gamma}$[b]	Error		$^{1}D_{C\alpha C\beta}$[c]	Error		$^{1}D_{C\beta H\beta}$[d]	Error	sum[e]	Error
3	TYR	Cγ	-2.63	0.35	Cα	1.61	0.07	Hβ#	5.21	0.82	-4.98	3.65
30	PHE	Cγ	-0.04	0.70	Cα	1.51	0.08	Hβ#	-18.45	0.46	-3.76	7.02
33	TYR	Cγ	0.16	0.19	Cα	0.19	0.06	Hβ#	-4.17	0.41	-0.70	2.07
35	ASN	Cγ	1.69	0.09	Cα	-0.58	0.06	Hβ#	-7.47	0.44	3.54	1.20
36	ASP	Cγ	-1.69	0.19	Cα	-1.12	0.06	Hβ#	22.51	0.32	-5.64	2.04
37	ASN	Cγ	0.87	0.29	Cα	0.57	0.05	Hβ#	-17.69	0.30	-3.34	2.96
39	VAL	Cγ1	1.14	0.03	Cα	0.07	0.04	Hβ	-25.33	0.24	-3.02	0.59
39	VAL	Cγ2	1.03	0.02								
40	ASP	Cγ	0.92	0.10	Cα	-0.07	0.04	Hβ#	-10.22	0.20	-1.71	1.13
42	VAL	Cγ1	-1.05	0.02	Cα	1.01	0.04	Hβ	0.86	0.57	-5.41	0.72
42	VAL	Cγ2	-0.59	0.02								
43	TRP	Cγ	1.70	0.35	Cα	-1.22	0.05	Hβ#	-5.02	1.93	-0.22	4.02
46	ASP	Cγ	0.02	0.17	Cα	-0.28	0.06	Hβ#	-0.22	1.19	-2.87	2.17
47	ASP	Cγ	-1.42	0.17	Cα	0.17	0.04	Hβ#	19.37	0.20	6.79	1.76
54	VAL	Cγ1	1.69	0.04	Cα	1.50	0.06	Hβ	-25.52	0.42	-3.31	0.92
54	VAL	Cγ2	-0.97	0.03								
										RMS[f]	3.94	2.89

PEG

Res#	AA type		$^{1}D_{C\beta C\gamma}$[b]	Error		$^{1}D_{C\alpha C\beta}$[c]	Error		$^{1}D_{C\beta H\beta}$[d]	Error	sum[e]	Error
3	TYR	Cγ	-0.87	0.17	Cα	0.99	0.07	Hβ#	-1.64	0.54	-0.45	1.93
6	VAL	Cγ1	-1.22	0.01	Cα	0.99	0.06	Hβ	16.02	0.32	1.11	0.69
6	VAL	Cγ2	-1.26	0.01								
8	ASN	Cγ	-0.77	0.18	Cα	0.97	0.05	Hβ#	-3.68	0.31	-1.63	1.87
21	VAL	Cγ1	-0.38	0.01	Cα	-0.07	0.04	Hβ	0.66	0.14	-1.31	0.43
21	VAL	Cγ2	0.25	0.01								
22	ASP	Cγ	0.16	0.10	Cα	0.90	0.06	Hβ#	-12.10	0.27	-1.52	1.20
30	PHE	Cγ	-0.62	0.23	Cα	0.80	0.09	Hβ#	-3.61	0.34	-1.84	2.48
33	TYR	Cγ	0.62	0.10	Cα	-0.54	0.06	Hβ#	-2.04	0.29	-1.21	1.20
35	ASN	Cγ	0.56	0.04	Cα	0.46	0.05	Hβ#	-9.43	0.25	0.77	0.70
36	ASP	Cγ	0.00	0.07	Cα	-0.92	0.05	Hβ#	9.97	0.27	0.77	0.89
37	ASN	Cγ	0.58	0.08	Cα	-0.15	0.06	Hβ#	-0.85	0.26	3.46	1.02
39	VAL	Cγ1	0.81	0.01	Cα	-0.53	0.05	Hβ	-10.93	0.15	2.03	0.53
39	VAL	Cγ2	1.01	0.01								
40	ASP	Cγ	0.84	0.04	Cα	-0.63	0.04	Hβ#	-2.19	0.15	-0.04	0.62
42	VAL	Cγ1	-0.52	0.01	Cα	0.88	0.01	Hβ	4.08	0.29	-2.32	0.32
42	VAL	Cγ2	-1.00	0.01								
43	TRP	Cγ	0.90	0.18	Cα	0.08	0.06	Hβ#	-6.24	1.43	3.53	2.34
45	TYR	Cγ	-1.50	0.14	Cα	-0.12	0.08	Hβ#	18.72	0.45	2.53	1.65
46	ASP	Cγ	-0.04	0.09	Cα	0.67	0.07	Hβ#	-3.44	0.42	2.84	1.21
47	ASP	Cγ	-1.39	0.05	Cα	0.61	0.06	Hβ#	7.45	0.16	-0.39	0.83
52	PHE	Cγ	-0.63	0.15	Cα	0.84	0.09	Hβ#	1.24	0.51	3.31	1.86
										RMS	1.97	1.34

Pf1

Res#	AA type		$^{1}D_{C\beta C\gamma}$[b]	Error		$^{1}D_{C\alpha C\beta}$[c]	Error		$^{1}D_{C\beta H\beta}$[d]	Error	sum[e]	Error
3	TYR	Cγ	-1.65	0.19	Cα	-0.14	0.08	Hβ#	14.83	0.38	-3.04	2.13
6	VAL	Cγ1	-0.01	0.01	Cα	-1.85	0.06	Hβ	-5.44	0.27	1.72	0.72
6	VAL	Cγ2	2.58	0.03								
8	ASN	Cγ	0.47	0.09	Cα	-1.89	0.05	Hβ#	11.01	0.30	-3.21	1.10

21	VAL	Cγ1	0.71	0.01	Cα	-1.36	0.04	Hβ	-4.62	0.08	0.58	0.43
21	VAL	Cγ2	1.17	0.01								
22	ASP	Cγ	-0.94	0.09	Cα	-1.65	0.07	Hβ#	27.10	0.29	1.25	1.18
30	PHE	Cγ	2.47	0.31	Cα	-2.14	0.12	Hβ#	-4.55	0.56	-1.28	3.35
33	TYR	Cγ	-1.76	0.17	Cα	0.55	0.06	Hβ#	8.01	0.41	-4.10	1.83
35	ASN	Cγ	-0.11	0.04	Cα	-1.66	0.05	Hβ#	18.58	0.17	0.84	0.65
36	ASP	Cγ	-1.41	0.13	Cα	3.76	0.08	Hβ#	-20.43	0.35	3.04	1.60
37	ASN	Cγ	3.05	0.11	Cα	0.25	0.07	Hβ#	-30.73	0.64	2.31	1.45
39	VAL	Cγ1	-1.65	0.01	Cα	1.59	0.06	Hβ	7.33	0.11	-2.74	0.63
39	VAL	Cγ2	-0.95	0.01								
40	ASP	Cγ	-0.96	0.05	Cα	1.04	0.05	Hβ#	-0.01	0.13	0.83	0.69
42	VAL	Cγ1	-1.41	0.01	Cα	0.01	0.01	Hβ	-11.41	0.24	-1.86	0.32
42	VAL	Cγ2	2.36	0.02								
43	TRP	Cγ	-2.23	0.17	Cα	-0.98	0.07	Hβ#	28.71	1.24	-3.43	2.24
45	TYR	Cγ	4.00	0.22	Cα	-1.33	0.09	Hβ#	-21.10	0.32	5.60	2.40
46	ASP	Cγ	-1.17	0.08	Cα	-1.84	0.07	Hβ#	29.04	0.28	-1.10	1.12
47	ASP	Cγ	1.41	0.09	Cα	-1.88	0.06	Hβ#	3.82	0.23	-0.90	1.10
52	PHE	Cγ	-0.95	0.18	Cα	-1.93	0.11	Hβ#	28.92	0.48	0.17	2.19
										RMS	2.53	1.58

[a] The sum of C^{β}-related ^1D couplings for three media: bicelle, PEG and Pf1, in which the RDCs have been scaled to the ^1D_a(CH) alignment strengths of 18.80, 12.62, and 19.70 Hz, respectively. Only residues having four C^{β}-related one-bond RDCs available are listed.

[b] $^1D_{C\beta C\gamma}$ RDCs were measured from the ^{1}H-^{13}C CT-HSQC spectrum for aromatic $^{13}C_{\gamma}$, and from the non-CT ^{1}H-^{13}C HSQC spectrum for methyl $^{13}C_{\gamma}$.

[c] $^1D_{C\alpha C\beta}$ RDCs were measured from ^{1}H-^{13}C HSQC and HN(CO)CA spectra.

[d] The sum of $^1D_{C\beta H\beta 2}$ and $^1D_{C\beta H\beta 3}$ RDCs were measured from the CT-HN(COCA)CB spectrum.

[e] The weighted sum of C_{β}-related ^1D, using $(^1D_{C\beta C\gamma} + {}^1D_{C\alpha C\beta}) \times 10 + {}^1D_{C\beta H\beta}$.

[f] The RMS value of the weighted sum of C_{β}-related ^1D, which is about 0.21, 0.16 and 0.13 times ^1D_a(CH) for bicelle, PEG and Pf1, respectively.

Table S6. Experimental $^1J_{C\alpha C\beta}$ and $^1D_{C\alpha C\beta}$ for GB3 (Hz)

RES#	AA type	A [a]		B		C		D	
		$^1J_{C\alpha C\beta}$ [b]	error	$^1D_{C\alpha C\beta}$ [c]	error	$^1D_{C\alpha C\beta}$ [b]	error	$^1D_{C\alpha C\beta}$ [b]	error
1	MET	33.09	0.04			1.59	0.07	-0.13	0.08
2	GLN	35.34	0.03	1.47	0.05	1.20	0.05	-0.75	0.06
3	TYR	32.61	0.04	1.61	0.07	0.99	0.07	-0.14	0.08
4	LYS	33.77	0.05	0.66	0.08	0.73	0.08	-1.85	0.09
5	LEU	34.46	0.08	1.18	0.12	0.55	0.12	-1.80	0.14
6	VAL	34.98	0.04	1.38	0.06	0.99	0.06	-1.85	0.06
7	ILE	36.04	0.04	1.70	0.08	0.97	0.07	-1.88	0.08
8	ASN	42.29	0.03	2.00	0.05	0.97	0.05	-1.89	0.05
10	LYS	33.36	0.03	0.01	0.06	-0.68	0.05	2.46	0.07
11	THR	37.24	0.01	0.30	0.02	-0.36	0.01	-1.37	0.03
12	LEU	34.49	0.04	-0.82	0.06	0.34	0.06	-1.37	0.07
13	LYS	34.82	0.04	-0.52	0.06	0.24	0.06	-1.37	0.07
15	GLU	33.28	0.03	0.61	0.04	-0.03	0.04	-0.49	0.05
16	THR	38.21	0.03	0.90	0.04	0.30	0.04	-1.38	0.04
17	THR	36.30	0.03	0.59	0.04	-0.32	0.05	1.97	0.06
18	THR	37.26	0.02	1.28	0.04	0.53	0.04	0.98	0.05
19	LYS	34.96	0.04	0.85	0.05	0.10	0.06	3.16	0.08
20	ALA	33.70	0.03	-0.60	0.07	-0.88	0.05	3.89	0.06
21	VAL	33.01	0.03	-1.37	0.04	-0.07	0.04	-1.36	0.04
22	ASP	35.46	0.04	0.32	0.05	0.90	0.06	-1.65	0.07
23	ALA	33.51	0.03	1.96	0.05	1.18	0.05	-0.87	0.06
24	GLU	33.28	0.03	-0.38	0.05	0.44	0.05	-1.85	0.05
25	THR	36.52	0.04	-1.79	0.08	-1.40	0.06	3.37	0.08
26	ALA	33.30	0.03	0.98	0.05	0.54	0.05	-1.46	0.06
27	GLU	32.90	0.04	2.86	0.08	1.77	0.06	-0.48	0.07
28	LYS	33.01	0.04	-2.20	0.10	-0.48	0.07	-0.78	0.07
29	ALA	33.23	0.03	-0.15	0.06	-0.78	0.04	3.36	0.06
30	PHE	34.68	0.06	1.51	0.08	0.80	0.09	-2.14	0.12
31	LYS	33.19	0.04	1.65	0.07	1.38	0.06	-1.07	0.07
32	GLN	33.48	0.03	-1.91	0.05	-0.82	0.05	1.68	0.06
33	TYR	32.12	0.03	0.19	0.06	-0.54	0.06	0.55	0.06
34	ALA	33.14	0.03	2.82	0.06	1.64	0.05	-1.23	0.05
35	ASN	34.26	0.03	-0.58	0.06	0.46	0.05	-1.66	0.05
36	ASP	35.98	0.03	-1.12	0.06	-0.92	0.05	3.76	0.08
37	ASN	36.19	0.03	0.57	0.05	-0.15	0.06	0.25	0.07
39	VAL	34.42	0.03	0.07	0.04	-0.53	0.05	1.59	0.06
40	ASP	37.32	0.03	-0.07	0.04	-0.63	0.04	1.04	0.05
42	VAL	34.11	0.01	1.01	0.04	0.88	0.01	0.01	0.01
43	TRP	33.04	0.04	-1.22	0.05	0.08	0.06	-0.98	0.07
44	THR	36.86	0.03	-0.28	0.04	0.47	0.04	-1.39	0.05
45	TYR	32.93	0.05	-1.63	0.07	-0.12	0.08	-1.33	0.09
46	ASP	37.10	0.04	-0.28	0.06	0.67	0.07	-1.84	0.07
47	ASP	33.58	0.03	0.17	0.04	0.61	0.06	-1.88	0.06
48	ALA	33.31	0.03	0.52	0.06	0.77	0.05	-1.03	0.06
49	THR	39.14	0.03	-3.65	0.05	-1.67	0.05	-0.01	0.04
50	LYS	38.70	0.05	-0.69	0.07	-0.58	0.07	3.37	0.09
51	THR	36.55	0.04	-0.63	0.06	0.43	0.06	-1.74	0.07
52	PHE	33.23	0.06	1.02	0.07	0.84	0.09	-1.93	0.11
53	THR	36.78	0.03	0.83	0.06	0.84	0.05	-1.40	0.06
54	VAL	34.62	0.04	1.50	0.06	0.94	0.06	-1.88	0.07

55	THR	37.99	0.03	2.14	0.05	1.26	0.05	-1.73	0.06
56	GLU	33.95	0.03						

[a] A-D represent isotropic GB3 and GB3 in three liquid crystalline media: bicelle, PEG, and Pf1, respectively. $^{1}J_{C\alpha C\beta}$ and $^{1}D_{C\alpha C\beta}$ were measured from ^{1}H-^{13}C HSQC and HN(CO)CA spectra.
[b] $^{1}J_{C\alpha C\beta}$ or $^{1}D_{C\alpha C\beta}$ represents the average of ^{1}H-^{13}C HSQC and HN(CO)CA derived values
[c] $^{1}D_{C\alpha C\beta}$ is from HN(CO)CA only.

Table S7. Structural statistics for the deposited models

Conformational restraints	
H-bonding PMF restraints	34
Through H-bond C′-N J-coupling restraints	32
H^N-H^α ^3J coupling restraints	48
C′- C′ ^3J coupling restraints	39
Residual dipolar coupling restraints, N-H^N	1235
Residual dipolar coupling restraints, C^α-H^α	884
Residual dipolar coupling restraints, H^N-H^α	89
Residual dipolar coupling restraints, C′-C^α	588
Residual dipolar coupling restraints, C^α-C^β	154
Residual dipolar coupling restraints, C′-N	264
Residual restraint violations	
H-bonding PMF energies (kT)	-4.3
Through H-bond C′-N J-coupling restraints (Hz)	0.11
H^N-H^α ^3J coupling restraints (Hz)	0.29
C′- C′ ^3J coupling restraints (Hz)	0.11
Residual dipolar coupling restraints, N-H^N (average Q-factor)	0.078
Residual dipolar coupling restraints, C^α-H^α (average Q-factor)	0.077
Residual dipolar coupling restraints, H^N-H^α (average Q-factor)	0.045
Residual dipolar coupling restraints, C′-C^α (average Q-factor)	0.094
Residual dipolar coupling restraints, C^α-C^β (average Q-factor)	0.050
Residual dipolar coupling restraints, C′-N (average Q-factor)	0.111
Model quality	
Rmsd bond length (Å)	0.009
Rmsd bond angles (°)	1.1
Rmsd improper torsion angles (°)	2.1
MolProbity Ramachandran statistics	
Favored regions (%)	98.1
Allowed regions (%)	100.0
Disallowed regions (%)	0.0
Global quality scores	
MolProbity clashes/1000 atoms	6.0
PROCHECK G-factor	0.18
Model contents	
Ordered residue ranges	1-56
Total number of residues	56
BMRB accession number	25807
PDB ID code	2N7J

Table S8. Analysis of χ_1 rotamer distributions in GB3

Res	N_{RDC} [a]	Model [b]	P [c]	$\rho(1)$ [d]	$\sigma_\rho(1)$ [e]	$\bar{\chi}_1(1)$ [f]	$\sigma_{\chi 1}(1)$ [g]	$\rho(2)$ [d]	$\bar{\chi}_1(2)$ [f]	$\sigma_{\chi 1}(2)$ [g]	$\rho(3)$ [d]	$\bar{\chi}_1(3)$ [f]	χ_1 [i] i	ii	iii	iv	v	vi	vii	viii	ix
M1	11	2	$<10^{-4}$	0.53	0.04	306	12	0.47	203	15	-	-	-		-80	-164	-76	-	-72	-142	-144
Q2	10	2	$<10^{-4}$	0.69	0.02	176	5	0.31	265	11	-	-	-		176	-62	-61	-67	-71	-60	-59
Y3	15	1	0.59	1.0	-	298	1	-	-	-	-	-	-66	-66	-60	-66	-61	-61	-62	-63	-64
K4	8	2	$<10^{-4}$	0.67	0.02	183	3	0.33	293	5	-	-	178	179	170	-173	-66	-72	172	-58	-61
L5	7	1	0.98	1.0	-	173	1	-	-	-	-	-	176	178	175	175	176	174	176	175	176
V6	11	1	0.89	1.0	-	178	1	-	-	-	-	-	172	174	-60	-53	-63	-53	-59	-64	-65
I7	10	1	0.39	1.0	-	299	1	-	-	-	-	-	-47	–54/ –168	-57	-67	-58	-64	-55	-68	-68
N8	12	2	$<10^{-4}$	0.58	0.01	190	2	0.42	296	3	-	-	-66	-67	-173	-168	-65	-63	177	-175	-176
K10	5	3	-	0.58	0.04	293	3	0.23	187	3	0.19	57	-81	-75	-75	-76	-72	-65	-57	-71	-77
T11	10	3	0.09	0.63	0.03	54	3	0.28	282	7	0.09	162	-102	66	-61	-151	-70	57	66	60	58
K13	10	3	0.005	0.67	0.02	302	2	0.16	62	12	0.16	160	-59	-57	-64	-63	-62	-172	-67	-71	-71
E15	8	3	0.004	0.44	0.01	285	3	0.34	40	4	0.22	163	-61	-65 / -39	-60	-58	-69	-172	179	-175	-175
T16	10	2	$<10^{-4}$	0.74	0.01	186	2	0.26	37	8	-	-	-172	-171	62	-52	-171	-61	-59	-170	-171
T17	10	2	$<10^{-4}$	0.76	0.01	65	1	0.24	195	7	-	-	66	67	67	66	61	-56	62	69	79
T18	10	1	0.10	1.0	-	197	1	-	-	-	-	-	-161	159	-162	-158	-162	68	64	-167	-168
V21	13	2	0.0002	0.60	0.05	302	3	0.40	68	4	-	-	-66	-65 / 75	-85	-70	62	-66	-66	-80	-76
D22	15	1	1.0	1.0	-	61	1	-	-	-	-	-	60	62	72	54	51	63	61	64	63
E24	10	2	$<10^{-4}$	0.53	0.02	284	6	0.47	182	5	-	-	97	178	-	-	-	-	-	-	-
E27	10	2	0.08	0.93	0.03	185	3	0.07	286	34	-	-	-177	-176	-168	-178	-164	-171	-176	-173	-172
K28	5	1	1.0	1.0	-	305	3	-	-	-	-	-	-80	-72	-76	-69	-56	177	-172	-68	-72
F30	15	1	0.35	1.0	-	289	1	-	-	-	-	-	-74	-71	-76	-71	-67	-76	-77	-75	-76
K31	10	2	$<10^{-4}$	0.84	0.01	285	2	0.16	181	9	-	-	-64	-74	-83	-77	-72	-79	-78	-76	-75
Q32	5	2	0.05	0.72	0.04	174	6	0.28	297	15	-	-	-177	-174	176	-57	179	177	178	-178	-177
Y33	14	1	0.009	1.0	-	179	1	-	-	-	-	-	165	166	177	168	-165	-69	-68	164	164

N35	15	2	$<10^{-4}$	0.52	0.01	184	2	0.48	288	3	-	-	-71	-171/ -69	-108	175	-174	-172	-177	-67	-68
D36	15	2	0.04	0.95	0.11	290	4	0.05	188	40	-	-	-73	-69	-71	-68	79	-73	-71	-80	-80
N37	15	1	1.0	1.0	-	285	1	-	-	-	-	-	-71	-72	-74	-73	-70	-65	-66	-72	-72
V39	15	2	$<10^{-4}$	0.83	0.02	178	2	0.17	324	9	-	-	171	173	177	-180	-72	177	172	174	178
D40[h]	15	2	$<10^{-4}$	0.69	0.13	179	11	0.31	237	15	-	-	179	-174	180	-176	-152	-63	-156	178	-165
V42	9	2	0.0005	0.83	0.02	171	1	0.17	35	6	-	-	-62	-63	-71	-74	-72	-68	-53	-72	-53
W43	11	1	1.0	1.0	-	287	1	-	-	-	-	-	-66	-68	-70	-73	-72	-70	-72	-68	-69
T44	10	2	0.001	0.84	0.02	48	1	0.16	270	6	-	-	62	63	72	71	63	65	70	65	67
Y45	15	1	1.0	1.0	-	178	2	-	-	-	-	-	174	175	174	173	177	-179	178	178	180
D46	15	2	0.0007	0.90	0.03	179	1	0.10	30	17	-	-	-176	-172	-172	-162	172	-177	-174	-174	-173
D47	15	2	$<10^{-4}$	0.82	0.02	189	3	0.18	98	12	-	-	-162	-162	-172	-161	-25	47	-163	-88	77
T49	10	1	1.0	1.0	-	63	2	-	-	-	-	-	63	65	61	68	59	66	66	68	66
K50	10	1	1.0	1.0	-	299	1	-	-	-	-	-	-48	-51	-58	-50	-62	-70	-46	-59	-59
T51	5	1	0.92	1.0	-	298	1	-	-	-	-	-	-58	-60	-61	-63	-60	-63	-58	-57	-57
F52	15	1	1.0	1.0	-	287	1	-	-	-	-	-	-68	-65	-68	-64	-70	-64	-63	-66	-66
T53	10	2	0.06	0.90	0.03	301	2	0.10	86	25	-	-	-53	-52	69	73	-58	86	-58	67	66
V54	15	2	0.0003	0.81	0.04	57	2	0.19	205	7	-	-	58	62	59	59	57	62	60	56	58
T55	6	1	0.06	1.0	-	303	1	-	-	-	-	-	-177	-174	-58	-55	-63	-62	-59	-73	-74
E56	9	2	$<10^{-4}$	0.56	0.02	286	7	0.44	184	8	-	-	-75	-66	-64	-70	-171	-165	-63	-76	-68

[a] N_{RDC} is the total number of experimental RDCs available for sidechain rotamer analysis with a maximum of 5 per vector, as the 6th RDC is a linear combination of the other 5.
[b] Model refers to the number of discrete χ_1 rotamers required to fit the data
[c] *P* refers to the probability, extracted from F statistics. For cases where model 1 is selected, *P* refers to the probability that model 1 is more applicable than model 2; for cases where model 2 is selected, *P* refers to the probability that model 2 is not better than model 1; for cases where model 3 is selected, *P* refers to the probability that model 3 is not better than model 2.
[d] Fractional population of rotamer (*n*)
[e] Uncertainty in fractional population of rotamer 1.
[f] χ_1 angle of rotamer (*n*)
[g] Uncertainty in χ_1 angle of rotamer (*n*)
[h] Values for this residue may be less accurate as they were derived under the assumption of a static C^{α}-C^{β} bond orientation, whereas the backbone of this residue is known to undergo substantial dynamics.[8,9]

[i] χ_1 angle of (i) 1IGD, (ii) 2IGD, (iii) 2GI9 (wild type GB1), (iv) 2QMT (GB1 with T2Q), (v) 2ZW0 (mutations D36E, N37H, D47P, A48E), (vi) 3FIL_ChainA (T2Q, E15V, T16L, T18I, N37L), (vii) 3FIL_ChainB (viii) 3MP9_ChainA (2 chains, A and B of wild type GB1) and (ix) 3MP9_ChainB. The red color indicates a residue type difference relative to wild type GB3; blue indicates a difference relative to the major rotamer determined by our NMR data.

Table S9. $^{3}J_{H\alpha\text{-}H\beta}$ in wild-type GB3

Res#	AA type	$^{3}J_{H\alpha\text{-}H\beta2}$ / Hz	$^{3}J_{H\alpha\text{-}H\beta3}$ / Hz
1	MET	5.8	6.1
2	GLN	5.4	8.0
3	TYR	10.5	3.1
4	LYS	6.4	8.0
5	LEU	5.3	11.8
6	VAL		9.6
7	ILE		10.1
8	ASN	6.3	7.1
11	THR		5.0
12	LEU	4.6	9.2
13	LYS	9.3	4.6
15	GLU	6.0	4.7
16	THR		2.2
17	THR		3.9
18	THR		3.1
20	ALA		5.8
21	VAL		4.1
22	ASP	4.2	2.8
23	ALA		6.8
24	GLU	6.6	6.9
25	THR		8.0
26	ALA		6.6
27	GLU	5.3	9.1
29	ALA		6.7
30	PHE	10.1	2.8
31	LYS	8.4	4.4
34	ALA		6.5
36	ASP	9.4	2.9
37	ASN	9.6	2.2
39	VAL		9.0
40	ASP	3.5	8.0
42	VAL		8.4
43	TRP	9.9	3.0
44	THR		3.2
45	TYR	6.3	11.6
46	ASP	4.0	9.8
47	ASP	4.3	10.2
48	ALA		7.1
51	THR		9.2
53	THR		8.0
54	VAL		4.2
55	THR		8.2

[a] Wild-type isotropic GB3, uniformly {^{13}C, ^{15}N}-enriched in 95% H_2O, 5% D_2O, 20 mM sodium phosphate buffer, 50 mM sodium chloride, pH 6.5, and 0.05% sodium azide. $^{3}J_{H\alpha H\beta}$ values were measured from a 600 MHz 3D HA[HN,HB](CACO)NH spectrum.

Table S10. $^3J_{H\alpha H\beta}$ Karplus equations for different types of amino acids[a].

Coupling type	A	B	C	D
Non-S/T/V-$^3J_{H\alpha H\beta 2}$	9.59	-0.99	0.58	1.22
Non-S/T/V-$^3J_{H\alpha H\beta 3}$	9.58	-0.98	0.31	1.22
Ser-$^3J_{H\alpha H\beta 2}$	8.55	-0.99	1.70	1.42
Ser-$^3J_{H\alpha H\beta 3}$	8.55	-0.99	0.81	1.42
Thr-$^3J_{H\alpha H\beta}$	7.14	-0.91	1.26	1.06
Val-$^3J_{H\alpha H\beta}$	8.58	-0.91	0.35	0.95

[a] A-D correspond to the coefficients in the Haasnoot-modified Karplus relation $^3J_{H\alpha H\beta}(\theta) = A\cos^2\theta + B\cos\theta + C\sin(2\theta) + D$

Table S11. Isotropic $^1J_{C\beta H\beta}$ for GB3 (Hz)

Res#	AA type	proton [a]	$^1J_{C\beta H\beta}$ [b]	Res#	AA type	proton [a]	$^1J_{C\beta H\beta}$ [b]
1	MET	Hβ2	131.6	31	LYS	Hβ2	129.3
1	MET	Hβ3	131.8	31	LYS	Hβ3	128.9
2	GLN	Hβ2		32	GLN	Hβ# [d]	132.4
2	GLN	Hβ3		33	TYR	Hβ2	130.7
3	TYR	Hβ2		33	TYR	Hβ3	127.5
3	TYR	Hβ3	126.9	35	ASN	Hβ2	131.6
4	LYS	Hβ2	129.4	35	ASN	Hβ3	130.4
4	LYS	Hβ3	128.1	36	ASP	Hβ2	131.3
5	LEU	Hβ2	130.8	36	ASP	Hβ3	125.3
5	LEU	Hβ3	126.4	37	ASN	Hβ2	128.9
6	VAL	Hβ	129.5 [c]	37	ASN	Hβ3	134.7
7	ILE	Hβ	128.6 [c]	39	VAL	Hβ	129.3 [c]
8	ASN	Hβ2	129.9	40	ASP	Hβ2	129.0
8	ASN	Hβ3	130.1	40	ASP	Hβ3	130.1
10	LYS	Hβ# [d]	128.9	42	VAL	Hβ	129.4 [c]
11	THR	Hβ	145.1	43	TRP	Hβ2	130.3
12	LEU	Hβ2	128.4	43	TRP	Hβ3	127.1
12	LEU	Hβ3	127.0	44	THR	Hβ	143.4
13	LYS	Hβ2	128.5	45	TYR	Hβ2	133.1
13	LYS	Hβ3	127.9	45	TYR	Hβ3	129.2
15	GLU	Hβ2 [e]	130.3	46	ASP	Hβ2	130.0
15	GLU	Hβ3 [e]	130.0	46	ASP	Hβ3	129.5
16	THR	Hβ	147.8	47	ASP	Hβ2	129.1
17	THR	Hβ	144.7	47	ASP	Hβ3	131.8
18	THR	Hβ	147.5 [c]	49	THR	Hβ	148.0 [c]
19	LYS	Hβ# [d]	130.4	50	LYS	Hβ2	130.7
21	VAL	Hβ	129.1 [c]	50	LYS	Hβ3	131.4
22	ASP	Hβ2	126.1	51	THR	Hβ	146.9 [c]
24	GLU	Hβ2	130.7	52	PHE	Hβ2	128.2
24	GLU	Hβ3	130.1	52	PHE	Hβ3	127.6
27	GLU	Hβ2	132.3	53	THR	Hβ	146.1 [c]
27	GLU	Hβ3	131.2	54	VAL	Hβ	131.8
28	LYS	Hβ# [d]	128.4	55	THR	Hβ	145.2 [c]
30	PHE	Hβ2	129.1	56	GLU	Hβ2	129.4
30	PHE	Hβ3	126.9	56	GLU	Hβ3	129.4

[a] $^1J_{C\beta H\beta}$ for stereospecifically assigned proton.

[b] $^1J_{C\beta H\beta}$ obtained from DEPT-filtered ^1H-^{13}C CT-HSQC by averaging the value from isotropic wild-type GB3 and three mutants (K4AK19EV42E-CHis$_6$, K19AV42ED47K and K4AK19EV42E) unless indicated otherwise.

[c] $^1J_{C\beta H\beta}$ is derived from the CT-HN(COCA)CB spectrum.

[d] # represents the two equivalent protons.

[e] ambiguous stereospecific assignment.

Table S12. Detected sum of $^1D_{C\beta H\beta 2}$ and $^1D_{C\beta H\beta 3}$ for GB3 (Hz)

RES#	AA type	A [a]		B		C		D		E		F	
		$^1D_{C\beta H\beta}$	error	$^1D_{C\beta H\beta}$	error	$^1D_{C\beta H\beta}$	error	$^1D_{C\beta H\beta}$	error	$^1D_{C\beta H\beta}$	error	$^1D_{C\beta H\beta}$	error
1	MET	6.95	0.69			10.16	0.52						
2	GLN	3.81	0.81	8.16	0.37	-5.26	0.49	-0.68	0.63	-2.58	0.57	6.59	0.54
3	TYR	9.23	1.02			-4.65	0.54	5.21	0.82	-1.64	0.54	14.83	0.38
4	LYS			10.39	0.75			9.00	0.87	0.52	0.57	14.20	0.53
5	LEU			-29.15	0.90			5.43	1.24	12.28	0.74	-13.93	0.82
6	VAL			-14.46	0.43	-5.07	0.41	24.37	0.47	16.02	0.32	-5.44	0.27
7	ILE	-10.70	0.65	-15.86	0.21	1.81	0.48	17.56	0.32	13.65	0.24	-5.39	0.21
8	ASN			10.26	0.30	6.67	0.41	-6.56	0.52	-3.68	0.31	11.01	0.30
10	LYS	-4.99	1.40	-16.65	0.41	7.37	0.87	-11.94	0.71	0.21	0.44	-20.44	0.61
11	THR	-6.09	0.33	-16.05	0.11	-1.06	0.16	13.32	0.21	10.35	0.13	-6.71	0.20
12	LEU	-17.62	0.61	9.79	0.35	-20.11	0.54	16.48	0.36	5.74	0.31	-8.70	0.25
13	LYS			14.31	0.31	-19.22	0.42	9.41	0.69	2.77	0.42	-7.63	0.33
15	GLU			-1.20	0.22			-9.08	0.66	-1.82	0.37	4.91	0.29
16	THR	11.12	0.25	19.74	0.12	4.11	0.18	-27.49	0.33	-15.36	0.19	-1.59	0.10
17	THR	6.92	0.49	13.83	0.17			-21.78	0.39	-11.39	0.20	-7.25	0.20
18	THR	18.84	0.38			3.98	0.20	-35.66	0.76	-23.11	0.28	10.34	0.16
19	LYS							-7.66	0.37	-1.08	0.31	-26.79	0.31
20	ALA	-17.09	1.11	-24.26	0.70	-3.24	0.58	3.70	2.24	10.70	0.80	-35.71	0.59
21	VAL	-7.51	0.17	8.94	0.12	-11.40	0.12	4.47	0.19	0.66	0.14	-4.62	0.08
22	ASP	23.00	0.70	20.27	0.30	-0.13	0.30	-12.01	0.38	-12.10	0.27	27.10	0.29
23	ALA	2.45	0.78	24.57	0.91	3.50	0.37	-18.34	0.54	-12.34	0.36	7.27	0.42
24	GLU	10.96	0.62	21.72	0.39	-2.19	0.35	-7.24	0.58	-9.12	0.39	18.17	0.29
26	ALA	12.71	2.03	8.40	0.68	2.00	0.74	-10.15	0.73	-5.40	0.49	13.65	0.78
27	GLU	-6.11	0.71	-10.97	0.73	5.78	0.43	-12.26	0.58	-2.60	0.37	-28.49	0.36
28	LYS	-3.93	0.62	28.01	0.38	-17.69	0.52	7.69	0.65	-3.91	0.40	18.36	0.25
29	ALA	-6.04	1.22	-28.22	0.68	2.63	0.71	1.71	0.69	9.69	0.51	-31.55	0.57
30	PHE	15.87	1.14	-7.99	0.60	14.25	0.63	-18.45	0.46	-3.61	0.34	-4.55	0.56
31	LYS	21.04	0.69	27.88	0.67	8.40	0.48	-31.08	0.63	-21.81	0.40	17.69	0.36
32	GLN	-12.47	0.77	15.91	0.41	-6.61	0.50	4.50	0.45	-0.52	0.36	2.69	0.31
33	TYR	13.84	1.05	-3.85	0.36	0.73	0.60	-4.17	0.41	-2.04	0.29	8.01	0.41
34	ALA	15.42	1.16	17.47	0.82	19.07	0.63	-24.68	0.67	-15.79	0.40	12.61	0.52
35	ASN	11.17	0.43	19.27	0.25	-5.53	0.24	-7.47	0.44	-9.43	0.25	18.58	0.17
36	ASP	-30.54	0.75	2.95	0.37	-23.11	0.37	22.51	0.32	9.97	0.27	-20.43	0.35
37	ASN	-0.36	0.98	-14.45	0.49	6.93	0.40	-17.69	0.30	-0.85	0.26	-30.73	0.64
39	VAL			2.24	0.14	16.99	0.27	-25.33	0.24	-10.93	0.15	7.33	0.11
40	ASP			-5.23	0.10	7.74	0.22	-10.22	0.20	-2.19	0.15	-0.01	0.13
42	VAL							0.86	0.57	4.08	0.29	-11.41	0.24
43	TRP					-2.84	1.57	-5.02	1.93	-6.24	1.43	28.71	1.24
44	THR	-9.35	0.38	24.59	0.19	-15.64	0.28	-4.26	0.46	-7.15	0.24	-5.77	0.20
45	TYR	-33.92	0.79	-9.67	0.43	-25.75	0.44	37.23	0.56	18.72	0.45	-21.10	0.32
46	ASP	16.30	0.73			-0.73	0.38	-0.22	1.19	-3.44	0.42	29.04	0.28
47	ASP	-10.02	0.33			-5.56	0.16	19.37	0.20	7.45	0.16	3.82	0.23
48	ALA	-1.92	1.18			-7.96	0.79	-4.92	1.17	-7.25	0.82	12.08	0.76
49	THR	-15.61	0.33	-16.38	0.25	-11.85	0.23	25.81	0.28	16.56	0.20	-11.26	0.14
50	LYS	-22.94	1.16			-0.75	0.71	30.25	0.93	23.65	0.75	-27.94	0.40
51	THR	-11.21	0.87			-11.90	0.60	25.46	0.61	15.58	0.47	-11.20	0.49
52	PHE			24.06	0.57	-15.80	0.64	16.84	0.90	1.24	0.51	28.92	0.48
53	THR	-11.93	0.65	-13.47	0.38	-8.38	0.44	20.51	0.43	13.34	0.33	-5.15	0.28
54	VAL			6.61	0.26	18.93	0.78	-25.52	0.42	-11.82	0.31	-2.43	0.27
55	THR			-15.06	0.37	0.08	0.35	16.21	0.43	13.21	0.31	-6.27	0.24

[a] A-C represent mutant 1 (K4A/K19E/V42E-CHis$_6$), mutant 2 (K19A/V42E/D47K), and mutant 3 (K4A/K19E/V42E) in Pf1, and D-F represent wild type GB3 in bicelles, PEG, and Pf1, respectively. The sum of $^1D_{C\beta H\beta 2}$ and $^1D_{C\beta H\beta 3}$ was measured from CT-HN(COCA)CB spectra.

Table S13. Detected individual $^1D_{C\beta H\beta 2}$ and $^1D_{C\beta H\beta 3}$ values for GB3 (Hz)

RES#	AA type	β proton	A [a]		B		C		D		E		F	
			$^1D_{C\beta H\beta}$ [b]	$^1D_{C\beta H\beta}$ [c]	$^1D_{C\beta H\beta}$ [b]	$^1D_{C\beta H\beta}$ [c]	$^1D_{C\beta H\beta}$ [b]	$^1D_{C\beta H\beta}$ [c]	$^1D_{C\beta H\beta}$ [b]	$^1D_{C\beta H\beta}$ [c]	$^1D_{C\beta H\beta}$ [b]	$^1D_{C\beta H\beta}$ [c]	$^1D_{C\beta H\beta}$ [b]	$^1D_{C\beta H\beta}$ [c]
1	MET	Hβ2	2.0	2.4	7.7	11.6	3.4	3.3	-10.4	-14.0			-0.3	-0.3
1	MET	Hβ3	2.5	3.0	-2.0	-3.1	3.7	3.6	-5.3	-7.1	-3.6	-4.0	2.8	2.7
2	GLN	Hβ2					-6.8	-6.6	1.9	2.5	-1.8	-2.0	18.2	17.6
2	GLN	Hβ3					-0.2	-0.2	-0.8	-1.0	0.4	0.5	-11.5	-11.1
3	TYR	Hβ2	-12.9	-15.5			-14.4	-14.0				0.0		
3	TYR	Hβ3	22.2	26.6			8.6	8.4	-7.9	-10.6	-9.5	-10.5	35.5	34.3
4	LYS	Hβ2			11.8	17.7			3.1	4.2	-3.9	-4.3	20.1	19.4
4	LYS	Hβ3			-1.4	-2.0			4.6	6.2	4.1	4.5	-6.3	-6.1
5	LEU	Hβ2			-9.7	-14.6					-6.1	-6.8	-12.2	-11.8
5	LEU	Hβ3			-9.1	-13.6					16.0	17.7	-0.6	-0.6
6	VAL	Hβ					-3.0	-2.9						
7	ILE	Hβ	-7.5	-9.0	-9.7	-14.6	4.7	4.6						
8	ASN	Hβ2			12.2	18.4	-1.7	-1.6	3.1	4.2	-4.5	-4.9	9.5	9.2
8	ASN	Hβ3			-5.4	-8.2	9.5	9.2	3.9	5.2	1.8	1.9	2.2	2.1
11	THR	Hβ	-4.1	-4.9	-7.7	-11.6	0.9	0.9	12.2	16.4	8.6	9.5	-6.5	-6.2
12	LEU	Hβ2	-7.5	-8.9	11.1	16.7	-16.8	-16.3	1.0	1.3	-1.5	-1.6	-8.5	-8.2
12	LEU	Hβ3	-4.1	-4.9	-3.4	-5.1	-2.7	-2.6	11.4	15.3	6.7	7.5	-1.9	-1.9
13	LYS	Hβ2			-3.9	-5.8	-4.3	-4.1	9.2	12.3	7.2	8.0	-5.3	-5.1
13	LYS	Hβ3			13.6	20.4	-15.3	-14.9	-3.1	-4.2	-3.5	-3.9	-2.9	-2.8
15	GLU	Hβ2 [d]			-0.7	-1.0			-1.6	-2.1	1.5	1.7	1.1	1.1
15	GLU	Hβ3 [d]			1.6	2.4			-5.5	-7.3	-2.0	-2.2	3.3	3.2
16	THR	Hβ	7.3	8.7	12.0	18.1	2.3	2.2	-20.6	-27.7	-12.5	-13.9	-2.2	-2.2
17	THR	Hβ	4.3	5.1	9.5	14.3			-17.6	-23.7	-10.3	-11.4	-8.2	-7.9
18	THR	Hβ	15.2	18.2			0.4	0.4					8.9	8.6
21	VAL	Hβ	-5.7	-6.8			-12.5	-12.1						
22	ASN	Hβ2	0.2	0.3			-4.8	-4.7	15.8	21.3	10.5	11.6	3.9	3.7
24	GLU	Hβ2	4.1	4.9	8.2	12.3	-2.8	-2.8	-2.4	-3.2	-3.2	-3.6	8.1	7.9
24	GLU	Hβ3	3.4	4.1	7.0	10.5	-2.0	-1.9	-3.0	-4.0	-4.8	-5.3	9.5	9.1
27	GLU	Hβ2	-10.9	-13.0	6.4	9.6	-17.9	-17.3	3.8	5.0	-0.6	-0.7	-17.1	-16.6
27	GLU	Hβ3							-12.1	-16.2	-0.4	-0.4		
30	PHE	Hβ2	-11.1	-13.3	-9.1	-13.6	-3.9	-3.8	11.5	15.4	11.9	13.2	-16.1	-15.6
30	PHE	Hβ3	21.3	25.5	3.0	4.4	19.1	18.5	-20.8	-28.0	-14.6	-16.1	12.7	12.2
31	LYS	Hβ2	16.5	19.8	1.1	1.7	12.9	12.5	-15.4	-20.7	-9.8	-10.9	4.8	4.6
31	LYS	Hβ3	-0.7	-0.8	17.4	26.2	-7.0	-6.8	-4.8	-6.4	-8.9	-9.8	13.2	12.7
33	TYR	Hβ2	22.6	27.1	9.5	14.3							24.1	23.2
33	TYR	Hβ3	-10.9	-13.0	-7.9	-11.9							-15.7	-15.1
35	ASN	Hβ2	3.4	4.1	5.7	8.5	-5.0	-4.9	-1.4	-1.9	-2.4	-2.6	5.6	5.4
35	ASN	Hβ3	4.3	5.1	9.5	14.3	-3.2	-3.1	-3.2	-4.3	-5.3	-5.9	12.0	11.6
36	ASP	Hβ2	-10.2	-12.2	8.8	13.3	-13.4	-13.1	0.4	0.6	-2.9	-3.2	-7.3	-7.1
36	ASP	Hβ3	-12.0	-14.4	-6.6	-9.9	-9.8	-9.5	14.8	19.9	13.3	14.7	-14.4	-13.9
37	ASN	Hβ2	-12.9	-15.5	3.2	4.8	-16.9	-16.4	2.4	3.2	3.8	4.2	-22.4	-21.6
37	ASN	Hβ3	10.6	12.7	-14.9	-22.5	23.4	22.7	-15.9	-21.3	-3.7	-4.1	-9.8	-9.4
39	VAL	Hβ					15.8	15.3		0.0				
40	ASP	Hβ2			-12.5	-18.7	-4.1	-4.0	10.1	13.6	8.5	9.4	-11.8	-11.4
40	ASP	Hβ3			9.5	14.3	10.0	9.7	-16.3	-21.9	-11.4	-12.6	12.1	11.7
43	TRP	Hβ2									14.5	16.1	-1.7	-1.7
43	TRP	Hβ3					-3.6	-3.5			-19.3	-21.4	30.7	29.7
44	THR	Hβ	-5.2	-6.2	16.5	24.9	-17.3	-16.8	-4.7	-6.4	-5.2	-5.8	-7.7	-7.5
45	TYR	Hβ2	-16.1	-19.2			-19.7	-19.1	4.7	6.3	2.1	2.3	-5.4	-5.2
45	TYR	Hβ3			-9.3	-14.0			20.2	27.2				
46	ASP	Hβ2	22.4	26.8			8.4	8.1	-17.2	-23.1	-17.2	-19.1	30.8	29.8
46	ASP	Hβ3	-8.8	-10.6			-9.0	-8.7	15.0	20.2	13.7	15.1	-2.8	-2.8
47	ASP	Hβ2	-0.7	-0.8			0.6	0.6	6.1	8.2	-0.8	-0.9	13.8	13.3
47	ASP	Hβ3	-6.8	-8.1			-7.3	-7.1	10.1	13.6	5.7	6.3	-11.4	-11.0

49	THR	Hβ	-10.9	-13.0	-9.3	-13.9	-9.6	-9.3	14.7	19.8	14.7	16.2	-11.4	-11.0
50	LYS	Hβ2	-11.6	-13.8			5.7	5.5	13.6	18.3	12.1	13.4	-7.4	-7.1
50	LYS	Hβ3	-7.9	-9.5			-4.5	-4.3			7.8	8.7	-20.0	-19.3
51	THR	Hβ	-7.9	-9.5			-11.7	-11.4	18.8	25.3	14.1	15.6	-11.5	-11.1
52	PHE	Hβ2			-8.4	-12.6	-9.5	-9.2	20.1	27.0	15.6	17.3	-3.4	-3.3
52	PHE	Hβ3			29.4	44.3	-5.7	-5.5	-8.6	-11.5	-15.0	-16.6	32.3	31.2
53	THR	Hβ					-5.6	-5.5					-4.5	-4.4
54	VAL	Hβ			3.6	5.4	13.1	12.7			-8.4	-9.3	-2.6	-2.5
55	THR	Hβ			-11.0	-16.6	2.1	2.1						
56	GLU	Hβ2			-6.3	-9.5	12.2	11.9	0.3	0.4	1.6	1.8	4.9	4.7
56	GLU	Hβ3			8.8	13.3	3.2	3.1	-8.3	-11.1			10.2	9.9

[a] A-C represent mutant 1 (K4A/K19E/V42E-CHis$_6$), mutant 2 (K19A/V42E/D47K), and mutant 3 (K4A/K19E/V42E) in Pf1, and D-F represent wild type GB3 in bicelles, PEG, and Pf1, respectively.

[b] The individual $^1D_{C\beta H\beta 2}$ and $^1D_{C\beta H\beta 3}$ were measured from DEPT-filtered ^{1}H-^{13}C CT-HSQC spectra.

[c] The individual $^1D_{C\beta H\beta 2}$ and $^1D_{C\beta H\beta 3}$ were scaled to the alignment strength of the sample used for the $^1D_{C\beta\text{-}H\beta}$ measurement from the CT-HN(COCA)CB spectrum.

[d] Ambiguous stereospecific assignment.

Table S14. Experimental $^{1}D_{C\beta C\gamma}$ values for GB3 (Hz)

RES#	AA type	γ carbon	A [a]			B			C			D			E			F		
			$^{1}D_{C\beta C\gamma}$ [b]	$^{1}D_{C\beta C\gamma}$ [c]	$^{1}D_{C\beta C\gamma}$ [d]	$^{1}D_{C\beta C\gamma}$ [b]	$^{1}D_{C\beta C\gamma}$ [c]	$^{1}D_{C\beta C\gamma}$ [d]	$^{1}D_{C\beta C\gamma}$ [b]	$^{1}D_{C\beta C\gamma}$ [c]	$^{1}D_{C\beta C\gamma}$ [d]	$^{1}D_{C\beta C\gamma}$ [b]	$^{1}D_{C\beta C\gamma}$ [c]	$^{1}D_{C\beta C\gamma}$ [d]	$^{1}D_{C\beta C\gamma}$ [b]	$^{1}D_{C\beta C\gamma}$ [c]	$^{1}D_{C\beta C\gamma}$ [d]	$^{1}D_{C\beta C\gamma}$ [b]	$^{1}D_{C\beta C\gamma}$ [c]	$^{1}D_{C\beta C\gamma}$ [d]
3	TYR	Cγ	0.2		0.2				0.0		0.0	-1.5		-2.6	-0.8		-0.9	-1.6		-1.6
6	VAL	Cγ1					0.0	0.0								-1.2	-1.2		0.0	0.0
6	VAL	Cγ2					2.9	3.9								-1.2	-1.3		2.5	2.6
7	ILE	Cγ2		0.7	0.7		3.2	4.2		-0.9	-0.9		-0.8	-1.4		-1.6	-1.7		2.3	2.4
8	ASN	Cγ							0.9		0.9				-0.7		-0.8	0.4		0.5
11	THR	Cγ2		1.2	1.1		1.4	1.8		0.2	0.2		-0.3	-0.5		-0.5	-0.5		1.8	1.9
16	THR	Cγ2		-0.7	-0.6		-0.4	-0.6		0.2	0.2		0.8	1.4		1.0	1.1		0.0	0.0
17	THR	Cγ2		0.0	0.0		-1.8	-2.4					-0.1	-0.1		0.6	0.6		-1.1	-1.2
18	THR	Cγ2		-1.4	-1.3					-1.0	-1.0		0.8	1.5		1.4	1.5		-1.1	-1.2
21	VAL	Cγ1		0.0	0.0											0.2	0.3		1.1	1.2
21	VAL	Cγ2		-0.1	-0.1		1.4	1.8		-0.5	-0.5		-0.1	-0.1		-0.4	-0.4		0.7	0.7
22	ASP	Cγ	-1.6		-1.5	-0.2		-0.3	-0.5		-0.5				0.1		0.2	-0.9		-0.9
25	THR	Cγ2		-1.5	-1.3														0.0	0.0
30	PHE	Cγ	0.4		0.3	1.8		2.3	-0.4		-0.4	0.0		0.0	-0.6		-0.6	2.4		2.5
33	TYR	Cγ	-0.6		-0.6	-1.7		-2.2	1.4		1.3	0.1		0.2	0.6		0.6	-1.7		-1.8
35	ASN	Cγ	-1.1		-1.0	0.0		0.0	-1.1		-1.0	0.9		1.7	0.5		0.6	-0.1		-0.1
36	ASP	Cγ	1.1		1.0	-1.7		-2.3	2.2		2.1	-0.9		-1.7	0.0		0.0	-1.4		-1.4
37	ASN	Cγ	1.1		1.0	-0.1		-0.1	0.4		0.4	0.5		0.9	0.6		0.6	2.9		3.1
39	VAL	Cγ1					-1.4	-1.8		-1.3	-1.3		0.6	1.1		0.8	0.8		-1.6	-1.7
39	VAL	Cγ2					-0.9	-1.2		0.6	0.6		0.6	1.0		1.0	1.0		-0.9	-0.9
40	ASP	Cγ				-0.8		-1.1	-0.1		-0.1	0.5		0.9	0.8		0.8	-0.9		-1.0
42	VAL	Cγ1											-0.6	-1.0		-0.5	-0.5		-1.4	-1.4
42	VAL	Cγ2											-0.3	-0.6		-1.0	-1.0		2.3	2.4
43	TRP	Cγ							-2.3		-2.2	0.9		1.7	0.9		0.9	-2.1		-2.2
44	THR	Cγ2		1.3	1.2		1.4	1.8		0.2	0.2		0.0	0.0		-0.6	-0.6		2.7	2.8
45	TYR	Cγ	3.1		2.8	2.8		3.7	-0.3		-0.3				-1.4		-1.5	3.8		4.0
46	ASP	Cγ	-1.6		-1.5				-2.2		-2.1	0.0		0.0	0.0		0.0	-1.1		-1.2
47	ASP	Cγ	2.0		1.8				0.6		0.6	-0.8		-1.4	-1.3		-1.4	1.4		1.4
49	THR	Cγ2		-1.1	-1.1		-1.8	-2.4		-0.3	-0.3					0.8	0.9		-2.0	-2.1
52	PHE	Cγ	1.4			-1.1		-1.4	1.6		1.6	-0.8		-1.4	-0.6		-0.6	-0.9		-0.9
53	THR	Cγ2		1.7	1.5		1.6	2.1		0.8	0.8		-1.4	-2.6		-1.6	-1.6		0.0	0.0
54	VAL	Cγ1					-0.7	-0.9		-0.9	-0.9		0.9	1.7		1.2	1.3		-0.2	-0.2
54	VAL	Cγ2					2.5	3.3		-0.3	-0.3		-0.5	-1.0		-1.0	-1.0		2.0	2.1
55	THR	Cγ2																	0.0	0.0

[a] A-C represent mutant 1 (K4A/K19E/V42E-CHis$_6$), mutant 2 (K19A/V42E/D47K), and mutant 3 (K4A/K19E/V42E) in Pf1, and D-F represent wild type GB3 in bicelle, PEG, and Pf1, respectively.

[b] $^{1}D_{C\beta C\gamma}$ was measured from a 900 MHz CT ^{1}H-^{13}C HSQC spectrum that left $^{13}C^{\beta}$-$^{13}C^{\gamma}$ dipolar and J coupling evolution intact.

[c] $^{1}D_{C\beta C\gamma}$ was measured from a 900 MHz real-time ^{1}H-^{13}C HSQC spectrum optimized for methyl ^{13}C evolution.

[d] $^{1}D_{C\beta C\gamma}$ was scaled to the alignment strength of the sample used for the $^{1}D_{C\beta H\beta}$ measurement, as measured from the CT-HN(COCA)CB spectrum.

Table S15. X values based on VW-Fit results

Res#	AA type	X^a		Number of RDCs [b]	Res#	AA type	X^a		Number of RDCs [b]
		$\delta H^{\beta 2} > \delta H^{\beta 3}$ / $\delta C^{\gamma 1} > \delta C^{\gamma 2}$	$\delta H^{\beta 3} > \delta H^{\beta 2}$ / $\delta C^{\gamma 2} > \delta C^{\gamma 1}$				$\delta H^{\beta 2} > \delta H^{\beta 3}$ / $\delta C^{\gamma 1} > \delta C^{\gamma 2}$	$\delta H^{\beta 3} > \delta H^{\beta 2}$ / $\delta C^{\gamma 2} > \delta C^{\gamma 1}$	
1	MET	2.45	1.73	11	31	LYS	8.34	0.97	12
2	GLN	2.02	3.84	10	32	GLN	0.70	0.70	6
3	TYR	0.86	7.84	15	33	TYR	1.36	5.89	15
4	LYS	1.06	7.05	8	35	ASN	1.47	1.07	18
5	LEU	1.51	10.09	7	36	ASP	5.71	1.37	18
6	VAL	7.34	1.19	11	37	ASN	1.01	12.45	18
7	ILE	0.81		12	39	VAL	2.18	1.35	15
8	ASN	0.61	4.85	13	40	ASP	1.99	2.53	15
10	LYS	1.60	1.60	6	42	VAL	1.97	0.78	9
11	THR	1.44		12	43	TRP	1.09	6.77	11
12	LEU	1.24	6.33	12	44	THR	0.87		12
13	LYS	0.72	7.05	10	45	TYR	7.96	2.25	17
15	GLU	0.78	1.07	8	46	ASP	1.20	7.82	15
16	THR	1.03		12	47	ASP	4.06	1.28	15
17	THR	0.86		10	49	THR	1.33		11
18	THR	1.51		10	50	LYS	5.44	0.88	10
19	LYS	0.00	0.00	3	51	THR	0.91		5
21	VAL	0.64	1.68	15	52	PHE	13.38	1.82	15
22	ASP	6.56	1.02	16	53	THR	1.07		12
24	GLU	1.26	1.15	12	54	VAL	7.86	1.92	15
27	GLU	11.89	2.04	12	55	THR	0.58		6
28	LYS	0.91	0.91	6	56	GLU	0.87	1.01	9
30	PHE	1.42	10.22	18					

[a] X values of VW-Fit results when using the backbone of the newly RDC-refined GB3 structure and the optimized entropy (the positive weight of the entropy term, θ, was adjusted such as to increase the total RDC component of the error function (eq 1) by 2% over not using this term).

[b] The number of RDCs used as input for VW-Fit.

Table S16. Observed and predicted (σ= 20°) $^3J_{Hα-Hβ}$ in wild-type GB3.

Res#	Res-Type	proton	$^3J_{HαHβ}$_obs / Hz	$^3J_{HαHβ}$_pred (σ = 20°) / Hz		$\Delta^3J_{HαHβ}$ (obs - pred) / Hz	
				1IGD	Rot-Analysis	1IGD	Rot-Analysis
1	Met	Hβ2	5.79		6.74		-0.95
1	Met	Hβ3	6.08		6.59		-0.51
2	Gln	Hβ2	5.37		5.41		-0.04
2	Gln	Hβ3	7.99		7.99		0.00
3	Tyr	Hβ2	10.51	10.52	10.61	-0.01	-0.09
3	Tyr	Hβ3	3.08	2.93	3.17	0.14	-0.09
4	Lys	Hβ2	6.35	4.28	5.91	2.07	0.44
4	Lys	Hβ3	8.03	10.66	8.06	-2.63	-0.03
5	Leu	Hβ2	5.29	4.50	4.82	0.79	0.46
5	Leu	Hβ3	11.80	10.62	10.48	1.18	1.32
6	Val	Hβ	9.61	9.24	9.53	0.36	0.08
7	Ile	Hβ	10.06	9.23	9.54	0.83	0.51
8	Asn	Hβ2	6.28	10.54	6.18	-4.26	0.10
8	Asn	Hβ3	7.13	2.97	7.36	4.16	-0.23
11	Thr	Hβ	4.98	4.54	3.71	0.44	1.27
13	Lys	Hβ2	9.28	10.72	8.81	-1.44	0.47
13	Lys	Hβ3	4.55	3.57	4.60	0.99	-0.05
15	Glu	Hβ2	4.85	10.69	6.37	-5.84	-1.52
15	Glu	Hβ3	6.01	3.37	5.27	2.64	0.74
16	Thr	Hβ	2.20	2.97	2.95	-0.77	-0.75
17	Thr	Hβ	3.94	2.34	2.51	1.59	1.43
18	Thr	Hβ	3.14	2.24	2.50	0.90	0.64
21	Val	Hβ	4.12	2.43	2.99	1.70	1.13
22	Asp	Hβ2	4.21	3.25	3.31	0.95	0.89
22	Asp	Hβ3	2.80	3.91	3.74	-1.11	-0.94
24	Glu	Hβ2	6.63	7.48	6.98	-0.85	-0.35

24	Glu	Hβ3	6.86	2.44	6.23	4.42	0.64
27	Glu	Hβ2	5.33	3.73	3.76	1.60	1.57
27	Glu	Hβ3	9.14	10.69	10.05	-1.55	-0.91
30	Phe	Hβ2	10.13	10.05	10.19	0.07	-0.06
30	Phe	Hβ3	2.80	2.46	2.49	0.34	0.31
31	Lys	Hβ2	8.35	10.60	8.90	-2.25	-0.56
31	Lys	Hβ3	4.43	3.10	3.65	1.33	0.78
36	Asp	Hβ2	9.45	10.11	10.23	-0.65	-0.78
36	Asp	Hβ3	2.90	2.50	2.53	0.40	0.37
37	Asn	Hβ2	9.56	10.21	9.87	-0.65	-0.31
37	Asn	Hβ3	2.25	2.57	2.26	-0.32	-0.01
39	Val	Hβ	8.95	9.21	8.85	-0.26	0.10
40	Asp	Hβ2	3.54	4.18	4.05	-0.63	-0.51
40	Asp	Hβ3	8.04	10.67	8.88	-2.63	-0.84
42	Val	Hβ	8.44	2.69	8.79	5.75	-0.34
43	Trp	Hβ2	9.93	10.51	10.02	-0.58	-0.09
43	Trp	Hβ3	3.04	2.92	2.36	0.13	0.68
44	Thr	Hβ	3.25	2.04	2.40	1.21	0.85
45	Tyr	Hβ2	6.26	4.76	4.24	1.50	2.02
45	Tyr	Hβ3	11.59	10.54	10.62	1.05	0.97
46	Asp	Hβ2	3.96	3.68	3.89	0.28	0.07
46	Asp	Hβ3	9.84	10.68	10.65	-0.84	-0.81
47	Asp	Hβ2	4.29	2.56	3.97	1.73	0.33
47	Asp	Hβ3	10.17	10.05	9.04	0.13	1.13
51	Thr	Hβ	9.16	8.34	8.38	0.82	0.78
53	Thr	Hβ	8.00	8.44	8.48	-0.44	-0.48
54	Val	Hβ	4.20	3.53	4.67	0.67	-0.47
55	Thr	Hβ	8.17	3.43	8.58	4.73	-0.41
RMSD						**2.05**	**0.75**

References

1. Ruckert, M.; Otting, G., *J. Am. Chem. Soc.* **2000,** 122, 7793-7797.
2. Fitzkee, N. C.; Bax, A., *J. Biomol. NMR* **2010,** 48, 65-70.
3. Lohr, F.; Schmidt, J. M.; Ruterjans, H., *J. Am. Chem. Soc.* **1999,** 121, 11821-11826.
4. Yamazaki, T.; Lee, W.; Arrowsmith, C. H.; Muhandiram, D. R.; Kay, L. E., *J. Am. Chem. Soc.* **1994,** 116, 11655-11666.
5. Silver, M. S.; Joseph, R. I.; Hoult, D. I., *Nature* **1984,** 310, 681-683.
6. Geen, H.; Freeman, R., *J. Magn. Reson.* **1991,** 93, 93-141.
7. Shaka, A. J.; Keler, J.; Freeman, R., *J. Mag. Res.,* **1983,** 53, 313-340.
8. Hall, J. B.; Fushman, D., *J. Biomol. NMR* **2003,** 27, 261-275.
9. Yao, L.; Vogeli, B.; Torchia, D. A.; Bax, A., *J. Phys. Chem. B* **2008,** 112, 6045-6056.